Single-family residential reconstruction after disasters: Building Permits Survey data and synthetic controls

Jack W. Baker[1], Nikola Blagojević[2], and Shujun Zhang[3]

[1]Professor, Dept. of Civil and Environmental Engineering, Stanford University, Stanford, CA 94305 (corresponding author). Email: bakerjw@stanford.edu
[2]Postdoctoral Scholar, Dept. of Civil and Environmental Engineering, Stanford University, Stanford, CA 94305. Email: nikolab@stanford.edu
[3]Graduate researcher, Dept. of Civil and Environmental Engineering, Stanford University, Stanford, CA 94305. Email: zhang123@stanford.edu

ABSTRACT

Understanding how quickly and completely communities rebuild after disasters is critical for recovery planning, yet systematic measurement of post-disaster reconstruction remains elusive. We use U.S. Census Bureau Building Permits Survey data to measure how disasters affect single-family residential new construction. For each disaster-affected place, we construct a synthetic control using weighted combinations of non-disaster places from the Building Permits Survey in the same Census region. Divergence between actual and synthetic permit activity after the event reveals the disaster's causal effect on new construction. We analyze 18 disasters that occurred between 2004 and 2023, including wildfires, hurricanes, and tornadoes. Wildfires produce large, sustained increases in permitting, with a median peak of more than five times the synthetic control, persisting for several years. Tornadoes produce moderate increases of roughly two times the counterfactual. Hurricanes—even those causing hundreds of millions of dollars in housing damage—produce a more modest average increase in new construction permits. We attribute these differences to the nature of the damage: wildfires and tornadoes tend to destroy structures completely, requiring new construction (and a new building permit), whereas hurricanes more often cause repairable damage, so recovery activity is less apparent in new construction data. These findings help quantify the timing and magnitude of new construction across a range of geographies and disaster types, and clarify the scope within which building permits data can serve as a proxy for post-disaster housing recovery.

PRACTICAL APPLICATIONS

When a disaster strikes a community, understanding of how quickly homes are being rebuilt is invaluable, but reliable, timely data on reconstruction progress has historically been scarce. This study shows that data from the U.S. Census Bureau's Building Permits Survey, which is publicly available, free, and updated monthly for thousands of communities nationwide, can serve as a practical tool for tracking post-disaster housing reconstruction. By comparing permit activity

in disaster-affected communities against what would have been expected without the disaster, it is possible to detect and measure reconstruction activity above normal background patterns. The study finds that the strength of this signal depends strongly on disaster type: wildfires and tornadoes, which tend to destroy homes completely, generate large and sustained increases in new construction permits; hurricanes, which more often cause repairable damage, produce more modest and variable increases. For wildfires in particular, permit surges typically peak one to two years after the event and persist for three to four years, which can inform resource planning, contractor capacity, and cost projections for recovery programs. These findings suggest that recovery agencies and insurers could use building permit data as a low-cost monitoring tool following future disasters where a large portion of damage is outright destruction.

INTRODUCTION

Disaster resilience research has matured unevenly. Hazard characterization benefits from decades of investment in seismic networks, weather radar, and remote sensing. Damage estimation is supported by large-scale experiments, numerical modeling, insurance loss databases, and rapid post-event assessments (National Research Council 2012). Recovery, by contrast, remains the least understood phase of the disaster cycle (Smith and Wenger 2007; Chang 2010; Cutter 2016). Housing recovery in particular is a process of extreme collective uncertainty that unfolds over years (Johnson and Olshansky 2017), and insufficient data remains a key barrier to effective recovery outcomes (Triveño et al. 2025). There is no national database that tracks how quickly damaged housing is restored, no standardized methodology for measuring the pace of reconstruction, and no longitudinal system for comparing recovery trajectories across events (National Academies of Sciences, Engineering, and Medicine 2019).

This measurement gap has practical consequences. A generation of computational models now attempts to forecast community recovery trajectories (Nejat and Damnjanovic 2012; Sutley and Hamideh 2018; Sutley and Hamideh 2020; Costa et al. 2021; Wang and van de Lindt 2021; Blagojević and Stojadinović 2022). These models have increasingly refined conceptual frameworks, but empirical reconstruction data to calibrate and validate their predictions remains limited. The recovery functions embedded in resilience quantification frameworks were originally proposed as mathematical concepts rather than as fits to observed data (Bruneau et al. 2003; Cimellaro et al. 2010; Sharma et al. 2020). When Aghababaei et al. (2020) attempted to validate an agent-based model against observed recovery data from the 2011 Joplin tornado, they found significant discrepancies between predicted and actual trajectories. Costa et al. (2024) concluded that longitudinal post-disaster data collection remains one of the most pressing needs for advancing recovery model validation. NIST has invested in longitudinal field studies to generate validation data (van de Lindt et al. 2020), but these labor-intensive efforts cover single communities and would benefit from supplementation with data from multiple disaster types and geographic contexts. The insurance and reinsurance industry faces a related need: catastrophe models incorporate the post-disaster spike in construction costs ("demand surge"), but the empirical basis for calibrating reconstruction pace and its effect on costs remains thin (Hallegatte 2008; Olsen and Porter 2011; Döhrmann et al. 2017).

The U.S. Census Bureau's Building Permits Survey (BPS) is a promising candidate to fill this gap. BPS provides nationally standardized, publicly available monthly counts of new residential construction permits at fine geographic resolution (U.S. Census Bureau 2025a). Building permits are a well-established leading economic indicator, used by the Federal Reserve and Department of Housing and Urban Development to track the housing sector. Because every new residential structure requires a permit, BPS data capture the pace and location of new construction activity across the entire country. The national scope, monthly frequency, place-level geography, and

multi-decade history make BPS well-suited to longitudinal, cross-event recovery measurement that the field currently lacks.

Despite this potential, only a handful of studies have used building permits to study post-disaster reconstruction. Stevenson et al. (2010) demonstrated that geocoded building permits could track the spatial and temporal dimensions of physical recovery following Hurricane Katrina in coastal Mississippi, finding that pre-disaster damage levels strongly influenced the timing and location of rebuilding. Kates et al. (2006) used permit counts in New Orleans as evidence of the "rush to rebuild" after Katrina, noting that 38,000 permits were issued within ten months despite unresolved planning questions. Cheng et al. (2015) applied a quasi-experimental design to BPS data in Katrina-affected counties and showed that the choice of recovery framework—whether recovery is measured as "bouncing back" to pre-disaster levels or relative to a counterfactual trajectory—yields substantially different conclusions about whether a community has recovered. Cui et al. (2015) used ARIMA intervention models on county-level BPS data for three hurricanes and found that storm landfalls produced temporary or permanent reductions in new building permit growth rates, but no reconstruction-driven increases, consistent with hurricane damage primarily generating repair activity invisible to BPS. Lee et al. (2024) analyzed local permit and tax assessor data from California wildfires and found that the pace of transition from permit application to reconstruction completion was similar across three fire-impacted communities. Most directly relevant, Arneson et al. (2020) used county-level BPS data across 204 disaster-affected regions from 2007 to 2013, measuring reconstruction as the percentage change in residential permits between the two years before and after a disaster. They found that pre-disaster construction labor availability had a statistically significant positive effect on reconstruction levels. Their work used a simple pre/post comparison, however, and the goal was to predict permit changes from market conditions rather than to empirically characterize the permit response itself. Across these studies, three gaps remain: no study has used counterfactual methods to isolate the causal effect of a disaster on permit activity, no study has systematically compared permitting activity across disaster types, and prior analyses have operated at county or metropolitan scales that may poorly match disasters' spatial footprints.

This paper demonstrates that synthetic control methods applied to place-level BPS data can detect and quantify post-disaster construction responses, and that these responses differ by disaster type. We analyze wildfires, hurricanes, and tornadoes that occurred between 2004 and 2023. For each disaster-affected place, we construct a synthetic control from weighted combinations of other BPS places in the same Census region, providing a baseline that accounts for non-disaster construction trends, seasonality, and regional economic conditions (Abadie and Gardeazabal 2003; Abadie et al. 2010). We work at the BPS "place" level—individual cities, towns, and unincorporated county areas—rather than at the county or metropolitan level, achieving a tighter geographic match between the data and the disaster footprint. The study examines only single-family permits; multi-family construction follows different market dynamics and is not considered here.

DATA

Building Permits Survey

The U.S. Census Bureau's Building Permits Survey (BPS) collects monthly and annual counts of new privately-owned residential construction permits nationwide (U.S. Census Bureau 2025a; U.S. Census Bureau 2025b). Data are reported by structure type (1-unit, 2-unit, 3–4 unit, 5+ units) and include the number of buildings, housing units, and construction valuation. Geographic resolution extends to four levels: state, core-based statistical area (CBSA), county, and individual permit-issuing place.

We assembled a place-level monthly panel from text files published on the Census Bureau website, covering January 2000 through October 2025. The resulting panel contains 21,011 unique places and approximately 3.3 million place-month observations. In contrast, the BPS data at other geographic levels are more aggregated: roughly 3,000 unique counties, or roughly 400 Metropolitan and Micropolitan Statistical Areas. Within the places data, we focus on the single-family permit counts. There were more than 22 million single-family permits issued in the data set (Fig. S1).

Several features of the BPS data require attention for this analysis. First, BPS captures only permits for new residential construction. It does not include repair permits, renovation permits, or manufactured (mobile) housing (U.S. Census Bureau 2021). Second, the reporting is voluntary. Approximately half of permit-issuing places report monthly; the remainder report only annually. The Census Bureau imputes data for non-respondents using regional ratios (U.S. Census Bureau 2025b). Our analysis uses only the monthly reporters, since annual data lack the temporal resolution needed to capture reconstruction dynamics.

Third, revisions to the BPS system over time create discontinuities. The list of permit-issuing places was redesigned in 2015, dropping approximately 2,600 smaller places from the monthly sample. A subsequent expansion in 2022 added approximately 11,500 places. For places that were dropped in 2015 and re-added in 2022, this creates a gap in the time series from roughly January 2015 through December 2021. We preserve these gaps as missing values (not months with zero permits) in the analysis.

Fourth, the raw data files span five distinct format eras. We constructed a unique place identifier to support data processing across eras and harmonized place names to resolve minor variations in naming conventions resulting from annexations, incorporations, and reclassifications.

FEMA Individual Assistance data

We obtain county-level FEMA Individual Assistance (IA) data from the OpenFEMA API (Federal Emergency Management Agency 2025b). IA data include the number of valid housing assistance registrations and the total assessed housing damage (in dollars) for each county affected by a federally declared disaster. We use these data to select disaster-affected places based on the intensity of county-level impact.

To help identify hurricane-affected places, we computed the county-level IA registration rate: the number of valid IA housing registrations per county population. This metric captures the extent to which a disaster affected a county's residential population, independent of county size.

Damage assessment data

We use two data sources to characterize the nature of damage in selected disasters. The CAL FIRE Damage Inspection (DINS) data classifies the damage level (destroyed, major, minor, or affected) of structures affected by California wildfires (California Department of Forestry and Fire Protection 2025). The FEMA Historical Damage Assessment (HDA) database provides similar structure-level damage classifications for hurricanes and tornadoes (Federal Emergency Management Agency 2025a). These data are used to compare the distribution of damage states across disaster types and interpret the differing BPS permit responses.

METHODS

The analysis aims to quantify the extent to which a disaster increased construction activity above what would have occurred otherwise. Underlying trends, seasonality, and regional economic conditions prevent us from simply comparing pre- to post-disaster permit counts. We

address this using the synthetic control method (Abadie and Gardeazabal 2003; Abadie et al. 2010), which constructs a place-specific counterfactual estimate of permit activity in the absence of the disaster. The counterfactual is formed from a weighted combination of permit activity in unaffected "donor" places with similar pre-disaster trajectories. The disaster-affected place is referred to as a "treated" unit, borrowing standard terminology from the causal inference literature. Divergence between the treated place's actual permits and its synthetic control after the disaster date is interpreted as the causal effect of the disaster on construction activity.

We assess the statistical significance of the predictions through placebo tests: we apply the same procedure to places that were not affected by a disaster. If the method were merely picking up random fluctuations, placebo (non-disaster) places would show similar deviations from their synthetic controls to those of the treated (disaster-affected) places. Treated places that stand out from this placebo reference distribution provide evidence of a genuine disaster effect. The following subsections describe how disaster-affected places are selected, how the synthetic control is constructed, and how significance is assessed.

Disaster and place selection

We analyze major U.S. disasters occurring between 2004 and 2023. Disasters occurring between 2000 (the start of the BPS data) and 2004 lack sufficient pre-disaster data to calibrate a synthetic control. Disasters occurring after 2023 lack sufficient post-disaster months for analysis of reconstruction activity. Within the selected time window, we use FEMA Individual Assistance (IA) data to identify dates and locations of communities that may have experienced post-disaster reconstruction activities. The spatial scale and extent of reconstruction vary by disaster type, given differences in damage mechanisms and disaster footprints. The following subsections describe the selection criteria, and Table 1 summarizes the selected events and places.

We identified six wildfires that caused substantial residential housing destruction: the 2017 Tubbs Fire, 2017 Thomas Fire, 2018 Woolsey Fire, 2018 Camp Fire, 2021 Marshall Fire, and 2023 Lahaina Fire. For each fire, we manually identified the BPS places most directly affected, based on known damage footprints. Of the 11 identified candidate places, four (Paradise, Butte County, Ventura County, and Superior) have BPS data gaps that include the fire dates, preventing synthetic control analysis. Additionally, Ventura was excluded due to evidence of reporting inconsistencies: the entire 2018-2025 post-fire period has only 320 total reported single-family permits, fewer than the 453 permits the city reports issuing for fire reconstruction alone (Ventura 2026); moreover, the data have an unusual number of large spikes, with several months having 10 times as many permits as adjacent months. The permit data for these excluded places are shown in Figs. S16 and S17 for reference, but they are not further analyzed. These exclusions also mean that the Thomas Fire and Camp Fire were not considered at all. The remaining six fire-affected places were included in the analysis.

We identified two major tornado events during the study period: the 2011 Joplin, MO tornado and the 2013 Moore, OK tornado. Both caused extensive residential destruction in well-defined geographic areas with active BPS reporting.

Two earthquakes that caused notable housing damage during the study period were considered: the 2014 Napa earthquake and the 2019 Ridgecrest earthquake. However, both places have large BPS survey gaps that prevent analysis of permit changes. Napa has a gap from 2015 to 2021 (the six years after the earthquake), and Ridgecrest has a gap from 2004 to 2022 (14 years before and 3 years after the earthquake). Raw permit time series for these places are shown in the Supplemental Materials, for reference, but they were not considered further.

For hurricanes, we used county-level FEMA Individual Assistance (IA) registration rates to identify the most heavily affected places, given the large number of candidate events and places.

We first selected hurricanes with cumulative IA housing damage exceeding $150 million. For each qualifying hurricane, county registration rates were computed as IA registrations divided by the 2020 Census county population. Counties with a registration rate exceeding 15% were retained as heavily affected. Within each high-registration county, we identified all BPS places and applied two additional filters: the place must average at least two single-family permits per month over its full BPS record, and must have continuous (gap-free) monthly data for a window of four years before and two years after the hurricane date. Many places in the most affected counties had short or interrupted BPS records, or very little permit activity, making them unsuitable for studying permitting trends. These criteria produced 78 hurricane-place pairs.

Several places appear in the damage footprint of more than one hurricane during the study period (e.g., Beaumont and Jefferson County, TX were affected by both Rita in 2005 and Ike in 2008; numerous Louisiana parishes were affected by both Katrina in 2005 and Ida in 2021). For places with multiple disaster events, we retain only the earliest event in the study period and exclude the later events. This ensures that each place's pre-disaster period is uncontaminated by prior disaster effects, leaving cleaner data for constructing a synthetic control. Nineteen hurricane-place pairs were excluded by this criterion, leaving 59 hurricane-place pairs for analysis. The excluded events are labeled on the time series plots in the Supplemental Materials.

Table 1 summarizes the disaster events and associated places analyzed in this study, sorted by disaster category and then date.

Table 1. Summary of the 18 disaster events and 67 associated places analyzed. Each row represents one disaster; places are listed with state abbreviations. Events are organized by hazard category and sorted by date within each category.

Category	Disaster	Date	Places
Wildfire	Tubbs Fire	2017-10	Santa Rosa, Sonoma Co. (CA)
Wildfire	Woolsey Fire	2018-11	Malibu (CA)
Wildfire	Marshall Fire	2021-12	Louisville, Boulder Co. (CO)
Wildfire	Lahaina Fire	2023-08	Maui Co. (HI)
Tornado	Joplin Tornado	2011-05	Joplin (MO)
Tornado	Moore Tornado	2013-05	Moore (OK)
Hurricane	Bonnie & Charley	2004-08	Charlotte Co., Hardee Co., Punta Gorda (FL)
Hurricane	Ivan	2004-09	Escambia Co., Pensacola (FL)
Hurricane	Katrina	2005-08	Grand Isle, Jefferson Par., Kenner, Mandeville, New Orleans, Ponchatoula, Slidell, St. Bernard Par., St. Charles Par., St. Tammany Par., Tangipahoa Par. (LA); Biloxi, Gautier, Gulfport, Harrison Co., Hattiesburg, Jackson Co., Long Beach, Ocean Springs, Pass Christian, Pearl River Co., Waveland (MS)
Hurricane	Rita	2005-09	Calcasieu Par., Jefferson Davis Par., Lake Charles, Sulphur, Vermilion Par. (LA); Beaumont, Cleveland, Dayton, Jefferson Co., Liberty Co. (TX)
Hurricane	Gustav	2008-08	Assumption Par., Terrebonne Par. (LA)
Hurricane	Ike	2008-09	Groves, Port Arthur (TX)
Hurricane	Isaac	2012-08	Plaquemines Par., St. John the Baptist Par. (LA)

Category	Disaster	Date	Places
Hurricane	Harvey	2017-08	Rockport, San Patricio Co. (TX)
Hurricane	Irma	2017-09	Islamorada, Marathon, Monroe Co. (FL)
Hurricane	Michael	2018-10	Bay Co. (FL)
Hurricane	Ida	2021-08	Covington, Lafourche Par., Livingston Par. (LA)
Hurricane	Ian	2022-09	Bonita Springs, Cape Coral, Estero, Fort Myers, Fort Myers Beach, Lee Co., Sanibel (FL)

Synthetic control method

For each disaster-affected place, we construct a synthetic control that estimates what the place's permit trajectory would have been in the absence of the disaster. The synthetic control method builds this counterfactual as a weighted combination of untreated "donor" units whose pre-treatment (pre-disaster) trajectories, when combined, closely match the treated unit (Abadie and Gardeazabal 2003; Abadie et al. 2010; Abadie 2021). The method has been applied to study the economic effects of disasters at the national level by Cavallo et al. (2013). Here we apply it to individual BPS places to isolate the causal effect of specific disasters on local construction activity.

The synthetic control for a treated place is a weighted combination of J donor places. Let Y_{1t} denote the outcome (single-family permits) for the treated place at time t, and Y_{jt} denote the same for donor j. The synthetic control is

$$\hat{Y}_{1t}^{\mathrm{SC}} = \sum_{j=2}^{J+1} w_j \, Y_{jt} \tag{1}$$

where $\hat{Y}_{1t}^{\mathrm{SC}}$ is the synthetic control estimate of Y_{1t}, $w_j \geq 0$ is the weight for donor j and J is the number of utilized donors. The treatment effect at time t is the difference $Y_{1t} - \hat{Y}_{1t}^{\mathrm{SC}}$.

For each disaster-affected (treated) place, we build a pool of potential donor places from the full BPS place-level panel, filtered to places in the same U.S. Census region but excluding the treated place's own state. We restrict donors to the same Census region (Northeast, Midwest, South, West) to ensure they share similar long-run economic and climatic conditions that drive broader residential construction trends, and exclude the treated place's own state to prevent contamination from nearby places that may have also experienced disaster effects. The within-state exclusion is particularly relevant for hurricanes, whose damage footprints can extend across many counties. All selected disaster-affected places are excluded from the donor pool, regardless of state. We also exclude places that average fewer than 2 single-family permits per month in the pre-period, as their low and volatile permit counts can produce unstable counterfactual predictions when amplified by the donor weights.

Donors must have data in the same months as the treated place's pre-disaster observations, and must also have continuous data for four years after the disaster date (or through the end of the study period, whichever is earlier). The pre-period requirement ensures that donor and treated data are directly comparable, and it naturally accommodates the survey gaps described earlier. The post-period requirement ensures that the synthetic control is constructed from donors that are continuously observed throughout the evaluation window, preventing artifacts from donor dropout.

For each disaster-affected place, the pre-disaster period extends from the earliest available data to the month before the first disaster event.

Synthetic control fitting

The synthetic controls are calibrated by selecting specific donors and fitting their weights, as defined in Eq. 1. From all eligible donors, we select the 200 most correlated with the treated place permits, measured by Pearson correlation on 12-month moving averages. Denoting the 12-month trailing moving average of any series Y_t as $\bar{Y}_t$, the moving average filters seasonality and month-to-month noise that degrades fitting, and the pre-filtering to 200 places keeps the optimization well-conditioned while retaining the most informative donors; the number of pre-filtered places was selected by iteratively increasing this value until the error metrics and number of donors with non-zeros weights stabilized.

We next use non-negative least squares to fit the weights in Eq. 1 by minimizing the sum of squared residuals between the treated place's moving average $\bar{Y}_{1t}$ and the weighted combination of donors' moving averages in the pre-disaster period only ($t = 1, \ldots, T_0$):

$$\min_{\mathbf{w} \geq 0} \sum_{t=1}^{T_0} \left(\bar{Y}_{1t} - \sum_{j=2}^{J+1} w_j \bar{Y}_{jt} \right)^2 \tag{2}$$

where $\mathbf{w} \geq 0$ denotes that all weights are restricted to non-negative values. Unlike Abadie et al. (2010), we do not constrain the weights to sum to one. Donor units often have significantly more or less permit activity than the target, so relaxing to unconstrained non-negative weights allows the synthetic control to match the treated unit at any scale, substantially improving fit quality.

The fitted weights are then applied to the donors' raw monthly permit counts for the full time range (pre- and post-disaster) to produce a synthetic control series that extends into the post-disaster period. A 12-month moving average of both the actual and synthetic series is computed for visualization and evaluation.

We assess fit quality using the root mean square prediction error (RMSPE) on 12-month moving averages in the pre-disaster period (Abadie et al. 2010; Abadie 2021):

$$\text{RMSPE} = \sqrt{\frac{1}{T_0} \sum_{t=1}^{T_0} \left(\bar{Y}_{1t} - \sum_{j=2}^{J+1} w_j \bar{Y}_{jt} \right)^2} \tag{3}$$

We express this as a percentage of mean pre-period permit activity (RMSPE%) to allow comparison across places with differing levels of permit activity.

For each disaster-affected place, we compute the cumulative excess permits as the sum of the difference between actual and synthetic monthly permit counts over the four years (48 months) following the disaster:

$$E = \sum_{t=T_0+1}^{T_0+48} \left(Y_{1t} - \hat{Y}_{1t}^{\text{SC}} \right) \tag{4}$$

Positive values indicate net new construction above the counterfactual baseline; negative values indicate suppressed construction. The 4-year summation window is chosen to capture the primary observed reconstruction period, while being short enough to limit extrapolation error in the synthetic control. For events with fewer than 4 years of post-disaster data, the sum is taken over all available months. Eq. 4 provides a simple scalar estimate of the total reconstruction signal in the BPS data.

Fig. 1 and later event plots show four time series for each place: raw monthly actual permits (thin blue line), raw monthly synthetic permits (thin gray line), 12-month moving average of actual (bold blue line), and 12-month moving average of synthetic (bold gray dashed line). Red

dashed vertical lines mark disaster events considered as treatments. Survey gaps appear as breaks in the actual series and are shaded in gray. The synthetic series is plotted continuously through gaps because the donor places have uninterrupted data. Synthetic predictions are displayed for up to eight years after the disaster event at each location, covering the recovery period, while avoiding decade-long extrapolations that lose predictive power.

Placebo inference

To assess the statistical significance of apparent trends in post-disaster permit activity, we conduct in-space placebo tests following the approach of Abadie et al. (2010). For each disaster event, we apply the same synthetic control procedure to randomly selected non-disaster places in the donor pool, using the same disaster date. If the disaster-affected places show genuinely anomalous permit behavior, their post-disaster prediction errors should be large relative to the distribution of placebo prediction errors.

We draw 10 placebo places from each of the seven states with a considered disaster (excluding Hawaii, which does not have 10 eligible places to contribute) and compute the post/pre RMSPE ratio for each.

Let T_1 denote the number of considered post-disaster months (here, 48 months). The ratio is defined as

$$R = \frac{\text{RMSPE}_{\text{post}}}{\text{RMSPE}_{\text{pre}}} = \frac{\sqrt{\frac{1}{T_1}\sum_{t=T_0+1}^{T_0+T_1}\left(\bar{Y}_{1t} - \sum_{j=2}^{J+1} w_j \bar{Y}_{jt}\right)^2}}{\text{RMSPE}} \tag{5}$$

where RMSPE is the pre-period fit error from Eq. 3. Note that even for placebo places with no disaster effect, the post/pre ratio is expected to exceed 1: the synthetic control weights are fit to the pre-period data, so the pre-period RMSPE reflects in-sample fit error, while the post-period RMSPE reflects out-of-sample prediction error on held-out data. The relevant question is therefore not whether the ratio exceeds 1, but whether the treated place's ratio is unusually large relative to the distribution of placebo ratios.

The same ratio is computed for all disaster-affected places, providing 70 values for the placebo places and 67 values for the disaster-affected places.

RESULTS

Across the 67 fitted places, the median pre-period RMSPE% is 5.7%, meaning the synthetic control typically matches actual permits to within about 6% of mean activity. The poorest fits tend to occur for Hurricane Katrina events, where training is hampered by having only 55 months of moving-average training observations before the August 2005 event date. Small places with few correlated donors (e.g., Louisville, CO) also have higher RMSPE%.

Fig. 1 shows the synthetic control pre-period fits for the places with the highest and lowest average pre-disaster permit volume. In both cases, the synthetic control closely tracks the actual permit series in the pre-disaster period, reproducing both the level and the seasonal pattern. The 12-month moving average fit is particularly close, as expected given that the weights are optimized on the moving averages. The raw monthly series shows more noise, but the synthetic control captures the central tendency well.

The Eq. 2 optimization assigns nonzero weight to a median of 13 donors per place, with a range 6 to 32 donors across places (Supplementary Fig. S2). But weight is concentrated: the top three donors typically carry approximately 80% of the total weight. Donors are geographically dispersed, drawn from a median of six states within the Census region. Supplementary Fig. S3 shows the percentage of each state's donors that come from each other state in the region.

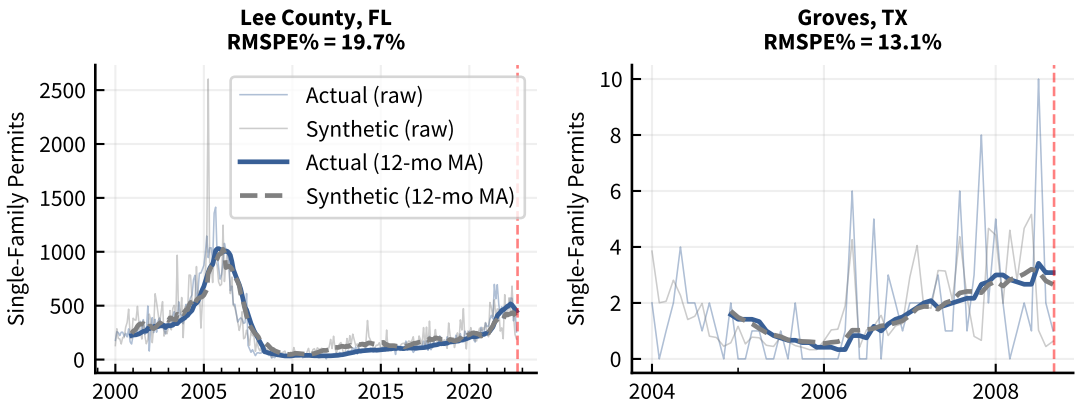

Fig. 1. Synthetic control pre-period fit for a high-activity place (left) and a low-activity place (right). Thin lines show raw monthly data; bold lines show 12-month moving averages. The red dashed line marks the pre-period cutoff (disaster date).

We next examine selected places affected by each disaster type, before proceeding to the aggregated analysis.

Wildfire-affected places

Fig. 2 shows patterns typical for wildfire-affected places. Permit activity remains unaffected or declines for a few months after the fire, reflecting the time required for debris removal and planning, and then rises substantially above the synthetic control within one to two years. This elevated permitting persists for several years as destroyed homes are rebuilt.

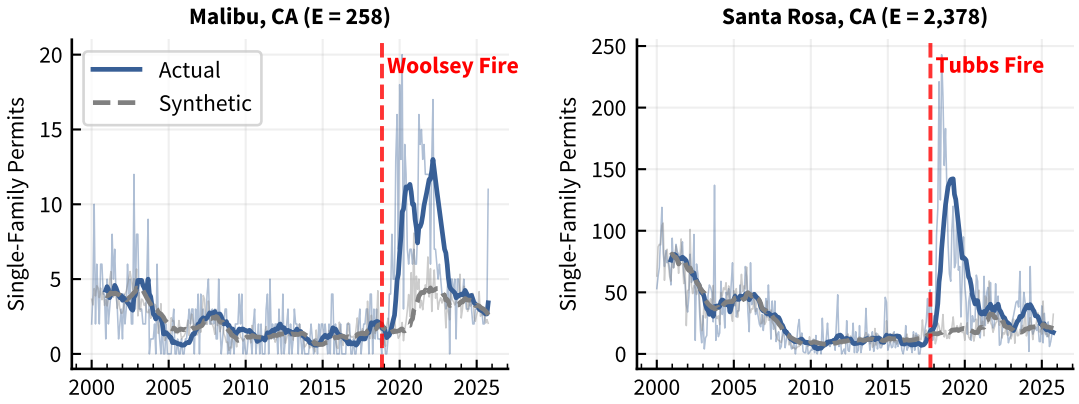

Fig. 2. Selected wildfire-affected places: actual vs. synthetic single-family permits. Thin lines show raw monthly data; bold lines show 12-month moving averages. Red dashed lines mark disaster dates. Individual time series for all wildfire places are shown in the Supplemental Materials.

The Woolsey Fire destroyed nearly 500 homes in Malibu (California Department of Forestry and Fire Protection 2025). Fig. 2 (left panel) shows a sharp post-fire surge in permits, with pre-fire permits of 1–2 per month rising to an average of about 10 per month for several years. As of early 2026, the City of Malibu reported 219 homes rebuilt and 308 permits issued (City

of Malibu 2026). The cumulative excess permits in the BPS data are 258 through four years, consistent with the local rebuilding permit count.

Santa Rosa, CA (Fig. 2, right panel), shows the response to the October 2017 Tubbs Fire, which destroyed 3,043 structures, of which 2,024 had a reconstruction permit within four years. The cumulative excess permits in the BPS data (2,378) exceed the count of reconstruction permits, likely reflecting two factors: Accessory Dwelling Units that were added during rebuilds (there were 114 permits for such ADUs over four years), and a broader fire-induced surge in new construction facilitated by streamlined citywide permitting adopted after the fire (Santa Rosa 2026).

Tornado-affected places

Fig. 3 shows results for the two tornado-affected places. The Joplin tornado destroyed more than 3,000 homes, and the Moore tornado destroyed 1,128 (Kuligowski et al. 2014a; Kuligowski et al. 2014b). Both places show an increase in single-family permits following the tornado, with a period when actual permits are well above the synthetic control. In Moore, the surge peaks approximately one year after the tornado, while in Joplin, the peak is nearly four years afterward.

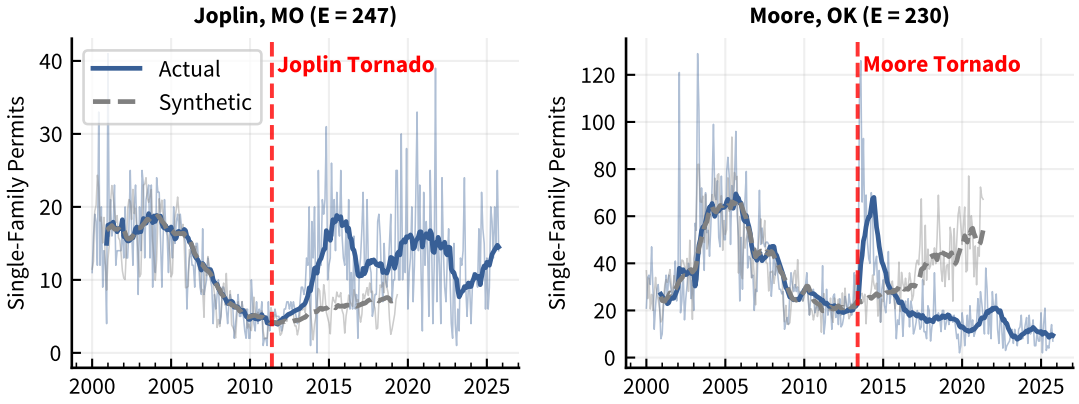

Fig. 3. Selected tornado-affected places: actual vs. synthetic single-family permits. Thin lines show raw monthly data; bold lines show 12-month moving averages. Red dashed lines mark disaster dates.

The excess single-family permits relative to the synthetic control are 247 for Joplin and 230 for Moore over the first four post-disaster years: a fraction of the homes destroyed in each event. Longitudinal field documentation of Joplin's recovery found that approximately 80% of tracked residential structures reached full functionality within two years (Pilkington et al. 2021), implying that most rebuilding occurred through repair rather than permitted new construction.

Hurricane-affected places

Fig. 4 shows four selected hurricane-affected places; individual time series for all 59 hurricane places are shown in Supplementary Figs. S6–S15. Despite substantial housing damage, permitting increases in hurricane-affected places are more mixed than in wildfire- and tornado-affected places.

Waveland, MS (Fig. 4, top left) is somewhat unusual among hurricane-affected places, showing a clear post-Katrina permit surge (with 362 excess permits). Waveland was located directly in the path of Katrina's approximately 30-foot storm surge on the Mississippi coast; the city's mayor estimated that 90% of the city was destroyed (NPR 2025). Bay County, FL (top

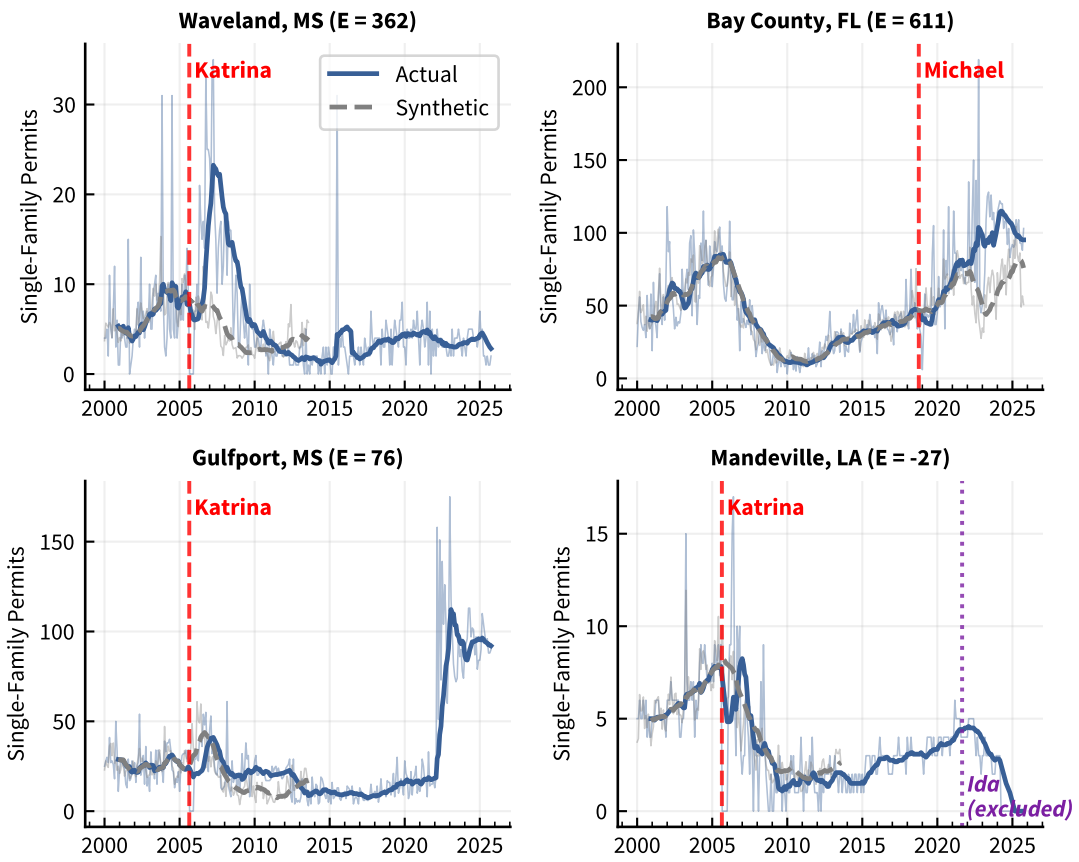

Fig. 4. Selected hurricane places: actual vs. synthetic single-family permits. Thin lines show raw monthly data; bold lines show 12-month moving averages. Red dashed lines mark disaster dates. Individual time series for all hurricane places are shown in the Supplemental Materials.

right) shows substantially elevated activity (611 excess permits) following Hurricane Michael, reflecting the approximately 1,500 structures the storm destroyed in the county (Beven et al. 2019). Gulfport, MS (bottom left), despite being in Harrison County with over 7,600 destroyed units county-wide, shows very little response (76 excess permits). Mandeville, LA (bottom right), located in St. Tammany Parish, was also affected by Katrina but shows no elevated permit activity (-27 excess permits, indicating essentially indistinguishable activity from the synthetic control).

Placebo tests

Fig. 5 shows two representative placebo places, illustrating how the synthetic control tracks the actual series both before and after the placebo treatment date, with no systematic deviation.

Fig. 6 shows the distribution of post/pre RMSPE ratios for placebo and disaster-affected places. Disaster-affected points are color-coded by disaster type. The median post/pre RMSPE ratio for disaster-affected places is 13.8, compared to a median of 5.7 for placebo places. This indicates that disaster-affected places experience substantially larger post-event deviations than would be expected by chance.

However, 20 of the 67 disaster-affected places (30%) have a ratio less than the placebo median ratio, indicating that not every disaster-affected place's response is individually distinguishable

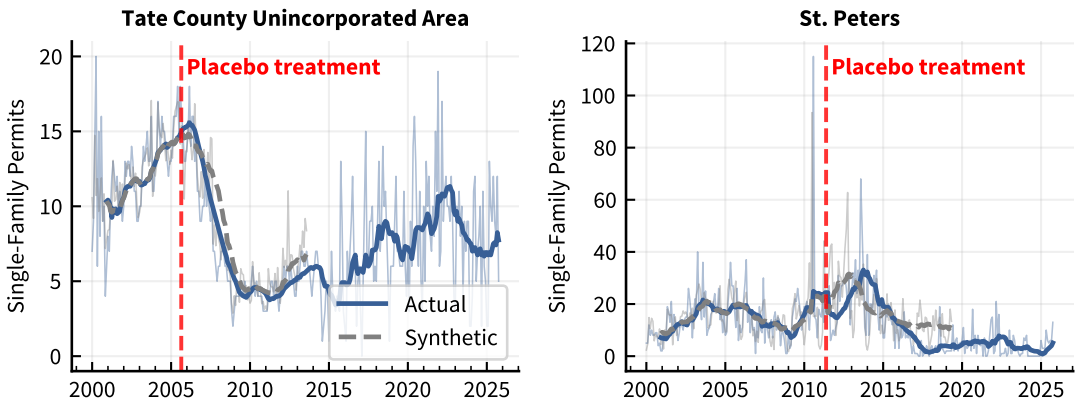

Fig. 5. Selected placebo places: actual vs. synthetic single-family permits. The red dashed line marks the placebo treatment date. The synthetic control tracks the actual series closely both before and after the treatment, as expected for non-disaster places.

from background noise. The overlap between the two distributions reflects the heterogeneity in disaster impacts: some disaster-affected places experienced relatively modest permit surges, while some placebo places, by chance, exhibit large swings in the post-period permit trend.

Average permitting trends

To summarize the across-event patterns, Fig. 7 shows normalized trends of permitting activities, aggregated by disaster type. For each place-event pair, we compute the ratio of the actual 12-month moving average to the synthetic control and plot this as a function of time relative to the disaster (years before and after the event). Values greater than 1 indicate higher permitting activity than predicted by the synthetic control. The vertical axis uses a logarithmic scale so that equal multiplicative changes receive equal visual weight (e.g., a doubling and a halving are equidistant from the baseline). Individual place traces are shown in light color; the bold line shows the median across places in each category. The fourth panel shows the placebo traces, providing a visual baseline for the natural variation expected in the absence of a disaster effect. The median trends from the four cases are then superimposed in Fig. 8 to facilitate comparison. Because each place contributes equally to the median, these summary results reflect the typical place-level response rather than the aggregate housing-weighted response.

Wildfires (top left) show a peak median ratio of more than 5 (i.e., actual permits more than 5 times the counterfactual), peaking one to two years after the fire and persisting for three to four years. Hurricanes (top right) show a median ratio that peaks at 1.5, modestly above the baseline and considerably below the wildfire and tornado responses; individual hurricane places vary widely. Tornadoes (bottom left) show a 2-fold increase in activity within six months of the disaster, with elevated activity through year 4, though general trends are unclear given that the results are based on only two places. Placebos (bottom right) have a median clustered tightly around 1, confirming that the median ratios for the disasters are well outside the range of normal fluctuation.

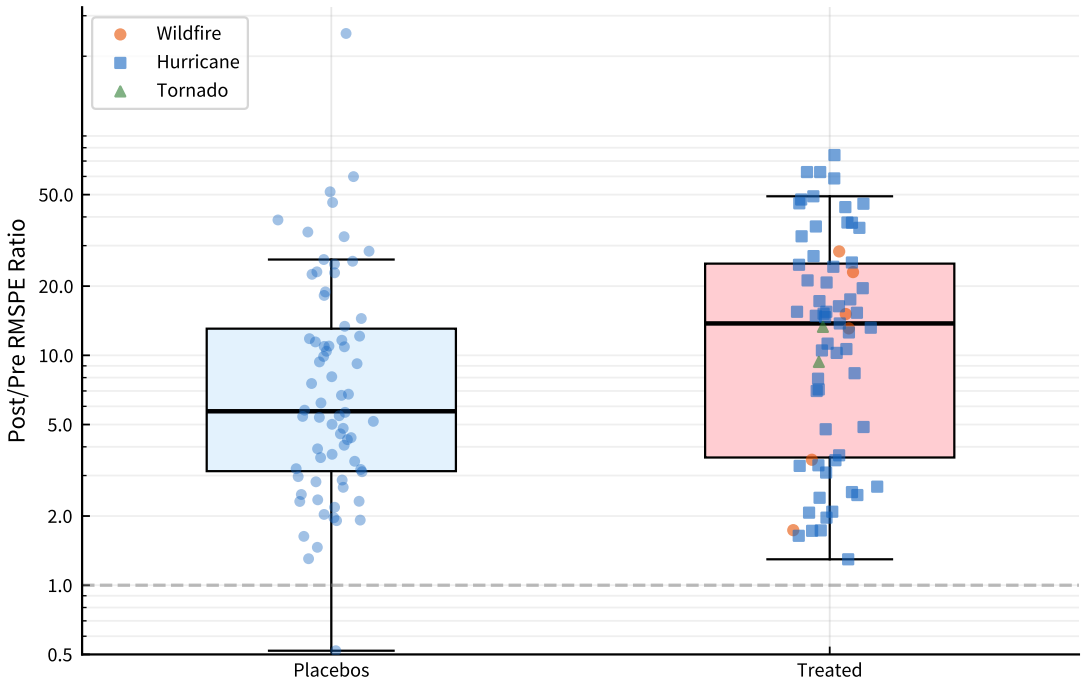

Fig. 6. Distribution of post/pre RMSPE ratios for placebo and disaster-affected (treated) places. Each point is one place; box plots summarize the distribution. Disaster-affected places are color-coded by disaster type. The dashed line marks a ratio of 1, indicating no change in prediction error after the event. Ratios above 1 indicate that post-event deviations exceed the pre-period baseline; higher values suggest a stronger departure from the synthetic control.

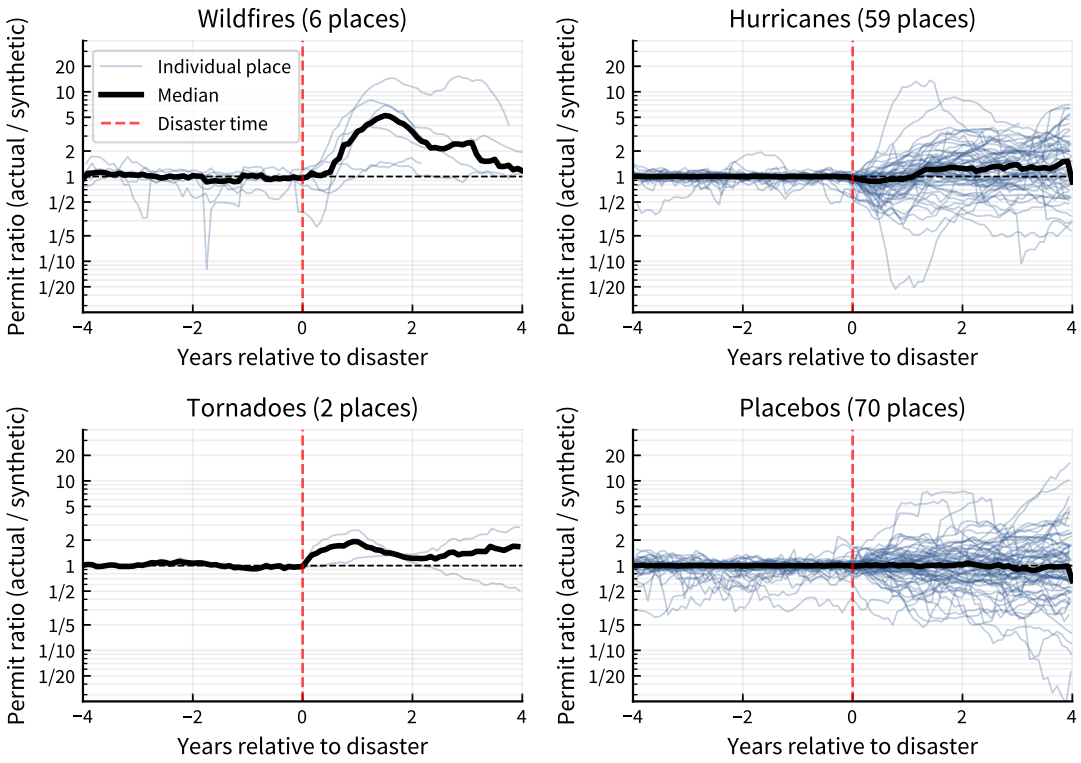

Fig. 7. Average permitting trends: ratio of actual to synthetic permits, aligned on disaster date. The vertical axis is logarithmic; a value of 1 means actual permits match the synthetic control. Each thin line is one place; the bold line is the median. The bottom-right panel shows placebo (non-disaster) places for comparison.

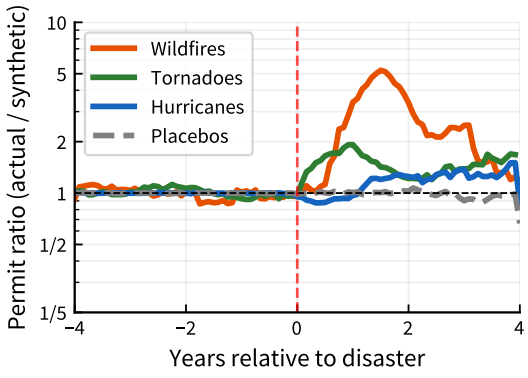

Fig. 8. Comparison of median permit ratios for the four cases in Fig. 7. The vertical axis is logarithmic; a value of 1 means actual permits match the synthetic control.

DISCUSSION

It is well established that the mode of disaster damage varies systematically across disaster types. Because BPS captures only new construction permits, Stevenson et al. (2010) noted that building permit data reflect only the "total loss" component of recovery. This implies that BPS should register a strong signal after events dominated by complete destruction, and a weaker signal after events dominated by repairable damage.

The results presented in this paper confirm those observations and quantify the gradient across 18 disasters and 67 places. Wildfires produce large, sustained increases in single-family permits (median peak ratio of more than 5 times the synthetic control). Tornadoes produce moderate increases. Hurricanes produce the smallest increases on average, though the large dataset shows significant variation from place to place.

This variation reflects not only the damage profile but also post-disaster economic dynamics. Santa Rosa's excess permits (2,378) exceed the number of fire-destroyed parcels rebuilt (2,024), suggesting that the fire catalyzed broader construction activity, facilitated in part by streamlined post-fire permitting. Conversely, places affected by Hurricane Katrina that experienced significant population loss, such as St. Tammany Parish and New Orleans, show suppressed or flat permit trends that reflect long-term demographic shifts rather than the absence of physical damage (Groen and Polivka 2010).

Damage assessment data further quantify the underlying mechanism. Fig. 9 shows the distribution of damage states for selected events, using CAL FIRE damage inspections for wildfires and the FEMA Historical Damage Assessment database for hurricanes and tornadoes (California Department of Forestry and Fire Protection 2025; Federal Emergency Management Agency 2025a). Note that the Thomas fire is used here for comparative context, to supplement the wildfire data, although it was not considered in the earlier analysis; the other nine events in the figure were analyzed earlier. Wildfires destroy the vast majority of affected structures: 81–96% of structures in the four California wildfires assessed were classified as destroyed. Tornadoes produce an intermediate profile, with 29–30% destroyed and an additional 12–21% sustaining major damage. Hurricanes produce predominantly light damage: 51–97% of assessed structures fall in the "Affected" (lightest) category, with fewer than 10% destroyed in the considered events. This gradient in damage state rates maps onto the gradient in BPS permit activity.

County-level damage data also reinforce the point. HUD damage estimates for Hurricanes Katrina and Rita (U.S. Department of Housing and Urban Development 2006) show overwhelmingly more damaged than destroyed housing units: Harrison County, MS had 41,033 units damaged versus 7,618 destroyed; St. Tammany Parish, LA had 47,130 damaged versus 1,682 destroyed; Calcasieu Parish, LA had 43,550 damaged versus 620 destroyed; and Jefferson County, TX had 45,482 damaged versus only 321 destroyed. For Hurricane Ian (2022), Lee County, FL had 24,585 units damaged and 5,369 destroyed (Lee County, Florida 2023). These damaged-to-destroyed ratios, ranging from roughly 5:1 to over 100:1, confirm that the vast majority of hurricane housing damage consists of repairable harm invisible to BPS. These figures are reported at the county or parish level, which generally encompass broader areas than the individual BPS places. Nonetheless, they indicate the predominant modes of damage.

More broadly, the proportion of structures destroyed in a disaster may serve as a practical indicator of whether BPS data will be informative for tracking recovery from a given event. Places with significant destruction rates, as observed for the wildfire-affected places in this study, produce permit surges that are large, sustained, and clearly distinguishable from background variation. Places with moderate destruction rates, such as the places affected by the two tornadoes, produce detectable but more moderate signals. Places dominated by repairable damage, as seen in most hurricanes, generate less BPS response. This suggests that early damage

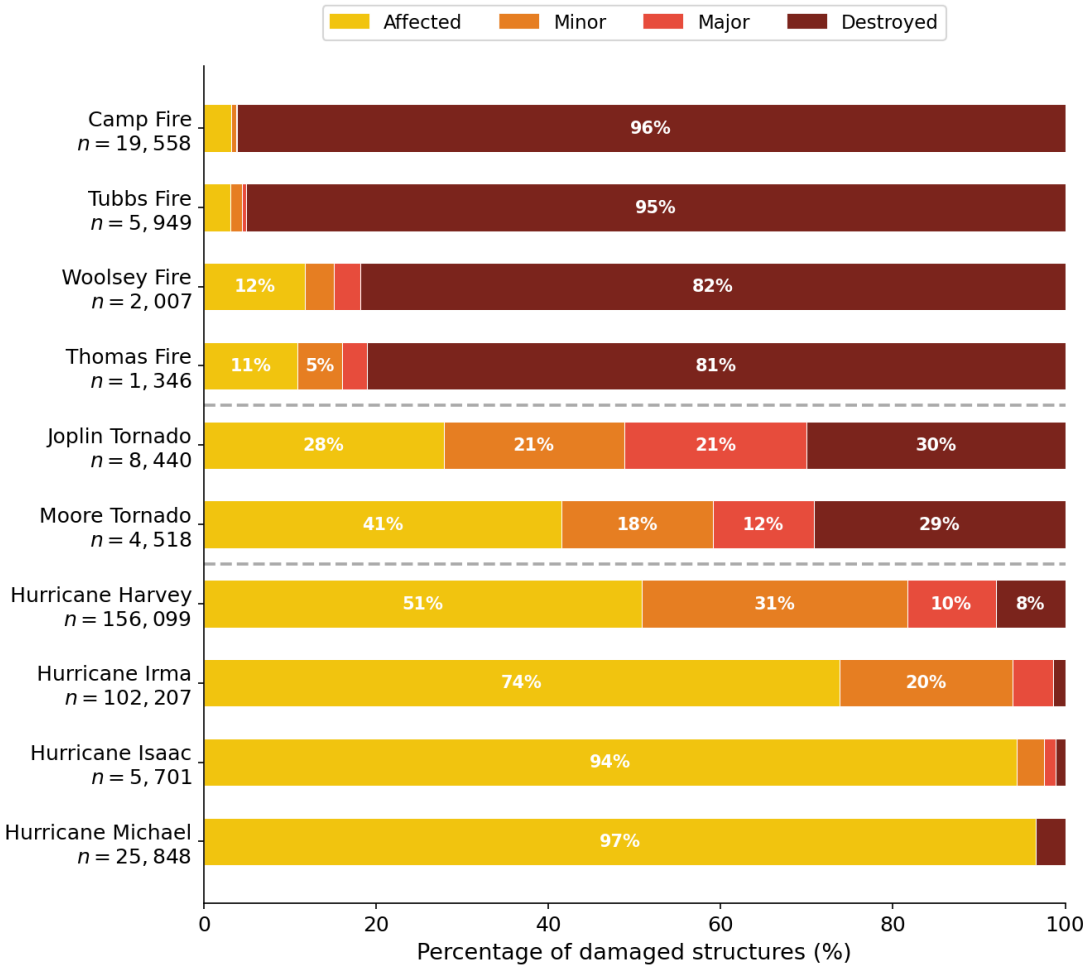

Fig. 9. Distribution of damage states for selected disaster events, excluding structures with no damage. Wildfire data from CAL FIRE damage inspections; tornado and hurricane data from the FEMA Historical Damage Assessment database. Sample sizes (n) are indicated in the labels.

assessments, such as those produced by CAL FIRE or FEMA's preliminary damage assessments within days of an event, could be used to judge prospectively whether BPS monitoring will yield useful recovery tracking information.

Several limitations of the analysis should be noted. First, although we draw donors from the same Census region while excluding the disaster-affected place's own state, some residual spatial correlation may remain. Large hurricanes may depress or stimulate construction activity across multiple states in a region, potentially affecting even out-of-state donors. This concern is substantially reduced compared with a same-state donor pool, where within-state spillover from a single hurricane is nearly unavoidable. Placebo tests (Section 5) provide further assurance: disaster-affected places show systematically larger post-event deviations than placebo places drawn from the same donor pool, confirming that the method detects genuine disaster effects above the noise floor. Second, the analysis considers only the new construction of single-family housing. Housing repairs, construction of manufactured (mobile) housing, and multi-unit housing are not considered. The analysis thus provides only a partial snapshot of the highly complex post-disaster reconstruction process. The share of housing stock that is single-family

varies regionally, meaning that the insights provided by this method will vary by context.

Future work could extend this analysis to incorporate multi-family permits, examine permit valuation (construction cost) rather than just counts to enable estimation of reconstruction expenditure, and link BPS data to supplemental data sources such as local repair permit records and tax assessor data. Applying this method prospectively to recent events, such as the 2025 Los Angeles wildfires or the 2024 Hurricanes Helene and Milton, would test whether the approach can support real-time reconstruction monitoring and forecasting, not just retrospective analysis.

CONCLUSIONS

This study demonstrates that synthetic control methods applied to place-level BPS data can detect and quantify post-disaster construction of destroyed houses. The method utilizes a place-specific counterfactual that accounts for pre-existing trends, seasonality, and regional economic conditions, without requiring explicit seasonal decomposition, consideration of construction dynamics between urban and rural areas, or the selection of a single comparison region. We analyze 18 disasters across 67 places, and find that the BPS permit response depends strongly on disaster type: wildfires and tornadoes, which tend to destroy structures completely, produce clear increases in new construction permits, while hurricanes produce on average a more modest increase.

These findings have several implications for disaster recovery research and practice. First, the stacked event results provide empirically grounded reconstruction curves that quantify the timing of the onset of increased activity, peak magnitude, and rate of decay. These parameters are directly relevant for computational disaster recovery models. For wildfire events in particular, these results appear to clearly indicate the timing and volume of recovery activity. For hurricanes, the average trend masks substantial heterogeneity: some places with high destruction rates (e.g., Waveland, Bay County) show large permit surges, while places where damage was predominantly repairable show little response. The new-construction data thus underestimate total recovery activity in most hurricane-affected places, though they can detect reconstruction where destruction was concentrated.

Second, the wildfire permit activity documented here—peaking at more than 5 times the pre-disaster baseline approximately 1–2 years after the event and persisting for 3–4 years—directly quantifies the construction demand spike that drives demand surge. These timing and magnitude estimates provide empirically grounded parameters for calibrating the pace and intensity of post-disaster construction demand.

Third, for events dominated by housing destruction, BPS data could serve as a near-real-time recovery tracker without requiring new data-collection infrastructure, since the data are free, nationally standardized, and updated monthly (with a three-month lag). However, for hurricanes and other mixed-damage events, modest BPS trends should not be interpreted as evidence that recovery is stalling. Recovery may simply be occurring through repair channels that are invisible to new-construction BPS permit data. Alternate data sources, such as local repair permit records, property tax assessments, or remote sensing, are needed to capture the scope of reconstruction in those cases. Those data sources have been successfully used following specific disasters, but the lack of a standardized national data set prevents the type of broad, cross-event study performed here.

Fourth, the study's 25-year BPS place-level panel of 21,011 places and 3.3 million observations is itself a contribution. Place-level BPS data have not previously been available in easily usable form for longitudinal analysis, and making this panel publicly available provides the research community with a curated, harmonized dataset for studying residential construction dynamics across a range of contexts.

DATA AVAILABILITY STATEMENT

All data used during the study are available from the sources cited above. The place-level BPS panel was assembled from publicly available Census Bureau Building Permits Survey files (U.S. Census Bureau 2025a). FEMA Individual Assistance data were obtained from the OpenFEMA API (Federal Emergency Management Agency 2025b). Wildfire damage inspection data were obtained from CAL FIRE (California Department of Forestry and Fire Protection 2025). Hurricane and tornado damage assessment data were obtained from the FEMA Historical Damage Assessment database (Federal Emergency Management Agency 2025a).

All code to assemble the data panel, perform the proposed analysis, and reproduce the paper figures is available at https://github.com/bakerjw/bps-disaster-permits.

ACKNOWLEDGMENTS

Support for this study was provided by the Stanford Urban Resilience Initiative. The Claude Opus 4.6 model was used to assist in developing the analysis code and in drafting and editing portions of the manuscript text. All output was reviewed and verified by the authors. The authors made all methodological, analytical, and editorial decisions, and take full responsibility for the content of this paper.

REFERENCES

Abadie, A. (2021). "Using synthetic controls: Feasibility, data requirements, and methodological aspects." *Journal of Economic Literature*, 59(2), 391–425.

Abadie, A., Diamond, A., and Hainmueller, J. (2010). "Synthetic control methods for comparative case studies: Estimating the effect of California's tobacco control program." *Journal of the American Statistical Association*, 105(490), 493–505.

Abadie, A. and Gardeazabal, J. (2003). "The economic costs of conflict: A case study of the Basque Country." *American Economic Review*, 93(1), 113–132.

Aghababaei, M., Koliou, M., Pilkington, S., Mahmoud, H., Van De Lindt, J. W., Curtis, A., Smith, S., Ajayakumar, J., and Watson, M. (2020). "Validation of Time-Dependent Repair Recovery of the Building Stock Following the 2011 Joplin Tornado." *Natural Hazards Review*, 21(4), 04020038.

Arneson, E., Javernick-Will, A., Hallowell, M., and Corotis, R. (2020). "Predicting Postdisaster Residential Housing Reconstruction Based on Market Resources." *Natural Hazards Review*, 21(1), 04019010.

Beven, J. L., Berg, R., and Hagen, A. (2019). "National Hurricane Center tropical cyclone report: Hurricane Michael (AL142018)." *Report no.*, National Hurricane Center. https://www.nhc.noaa.gov/data/tcr/AL142018_Michael.pdf. Accessed March 2026.

Blagojević, N. and Stojadinović, B. (2022). "A Demand-Supply Framework for Evaluating the Effect of Resource and Service Constraints on Community Disaster Resilience." *Resilient Cities and Structures*, 1(1), 13–32.

Bruneau, M., Chang, S. E., Eguchi, R. T., Lee, G. C., O'Rourke, T. D., Reinhorn, A. M., Shinozuka, M., Tierney, K., Wallace, W. A., and von Winterfeldt, D. (2003). "A framework to quantitatively assess and enhance the seismic resilience of communities." *Earthquake Spectra*, 19(4), 733–752.

California Department of Forestry and Fire Protection (2025). "Incident information. https://www.fire.ca.gov/incidents. Accessed March 2026.

Cavallo, E., Galiani, S., Noy, I., and Pantano, J. (2013). "Catastrophic natural disasters and economic growth." *Review of Economics and Statistics*, 95(5), 1549–1561.

Chang, S. E. (2010). "Urban disaster recovery: A measurement framework and its application to the 1995 Kobe earthquake." *Disasters*, 34(2), 303–327.

Cheng, S., Ganapati, E., and Ganapati, S. (2015). "Measuring disaster recovery: Bouncing back or reaching the counterfactual?." *Disasters*, 39(3), 427–446.

Cimellaro, G. P., Reinhorn, A. M., and Bruneau, M. (2010). "Framework for analytical quantification of disaster resilience." *Engineering Structures*, 32(11), 3639–3649.

City of Malibu (2026). "Woolsey fire rebuild statistics. https://malibupermits.ci.malibu.ca.us/WoolseyRebuildStats.aspx. Accessed March 2026.

Costa, R., Haukaas, T., and Chang, S. E. (2021). "Agent-based model for post-earthquake housing recovery." *Earthquake Spectra*, 37(1), 46–72.

Costa, R., Haukaas, T., and Chang, S. E. (2024). "Community seismic resilience for the building portfolio in Victoria, British Columbia." *Earthquake Spectra*, 40(1), 478–504.

Cui, Y., Liang, D., and Ewing, B. T. (2015). "Empirical Analysis of Building Permits in Response to Hurricane Landfalls." *Natural Hazards Review*, 16(4), 04015009.

Cutter, S. L. (2016). "The landscape of disaster resilience indicators in the USA." *Natural Hazards*, 80(2), 741–758.

Döhrmann, D., Gürtler, M., and Hibbeln, M. (2017). "An econometric analysis of the demand surge effect." *Journal of Risk and Insurance*, 84(3), 797–825.

Federal Emergency Management Agency (2025a). "Historical damage assessment database. https://www.fema.gov/about/openfema/data-sets. Accessed March 2026.

Federal Emergency Management Agency (2025b). "OpenFEMA data sets. https://www.fema.gov/about/openfema/data-sets. Accessed February 2026.

Groen, J. A. and Polivka, A. E. (2010). "Going home after Hurricane Katrina: Determinants of return migration and changes in affected areas." *Demography*, 47(4), 821–844.

Hallegatte, S. (2008). "An adaptive regional input-output model and its application to the assessment of the economic cost of Katrina." *Risk Analysis*, 28(3), 779–799.

Johnson, L. A. and Olshansky, R. B. (2017). *After Great Disasters: How Six Countries Managed Community Recovery*. Lincoln Institute of Land Policy, Cambridge, MA.

Kates, R. W., Colten, C. E., Laska, S., and Leatherman, S. P. (2006). "Reconstruction of New Orleans after Hurricane Katrina: A research perspective." *Proceedings of the National Academy of Sciences*, 103(40), 14653–14660.

Kuligowski, E. D., Lombardo, F. T., Phan, L. T., Levitan, M. L., and Jorgensen, D. P. (2014a). "Technical investigation of the May 20, 2013, Tornado in Moore, Oklahoma." *Special Publication 1164*, National Institute of Standards and Technology.

Kuligowski, E. D., Lombardo, F. T., Phan, L. T., Levitan, M. L., and Jorgensen, D. P. (2014b). "Technical investigation of the May 22, 2011, Tornado in Joplin, Missouri." *NCSTAR 3*, National Institute of Standards and Technology.

Lee, J., Costa, R., and Baker, J. W. (2024). "Post-Disaster Housing Recovery Estimation: Data and Lessons Learned from the 2017 Tubbs and 2018 Camp Fires." *International Journal of Disaster Risk Reduction*, 104912.

Lee County, Florida (2023). "Hurricane Ian after action report. Reported in Cape Coral Breeze, August 15, 2023. Accessed March 2026.

National Academies of Sciences, Engineering, and Medicine (2019). *Building and Measuring Community Resilience: Actions for Communities and the Gulf Research Program*. The National Academies Press, Washington, DC.

National Research Council (2012). *Disaster Resilience: A National Imperative*. The National Academies Press, Washington, DC.

Nejat, A. and Damnjanovic, I. (2012). "Agent-Based Modeling of Behavioral Housing Recovery

Following Disasters." *Computer-Aided Civil and Infrastructure Engineering*, 27(10), 748–763.

NPR (2025). "Waveland, Miss., is still recovering 20 years after Hurricane Katrina hit (August). https://www.npr.org/2025/08/25/nx-s1-5479158/waveland-miss-is-still-recovering-20-years-after-hurricane-katrina-hit. Accessed March 2026.

Olsen, A. H. and Porter, K. A. (2011). "What We Know About Demand Surge: Brief Summary." *Natural Hazards Review*, 12(2), 62–71.

Pilkington, S. F., Curtis, A., Mahmoud, H., van de Lindt, J., Smith, S., and Ajayakumar, J. (2021). "Preliminary Documented Recovery Patterns and Observations from Video Cataloged Data of the 2011 Joplin, Missouri, Tornado." *Natural Hazards Review*, 22(1), 05020015.

Santa Rosa (2026). "Resilient City Zoning Code & Map Amendment | Santa Rosa, CA.

Sharma, N., Tabandeh, A., and Gardoni, P. (2020). "Regional resilience analysis: A multiscale approach to optimize the resilience of interdependent infrastructure." *Computer-Aided Civil and Infrastructure Engineering*, 35(12), 1315–1330 Online 2019.

Smith, G. P. and Wenger, D. (2007). "Sustainable disaster recovery: Operationalizing an existing agenda." *Handbook of Disaster Research*, H. Rodríguez, E. L. Quarantelli, and R. R. Dynes, eds., Springer, 234–257.

Stevenson, J. R., Emrich, C. T., Mitchell, J. T., and Cutter, S. L. (2010). "Using building permits to monitor disaster recovery: A spatio-temporal case study of coastal Mississippi following Hurricane Katrina." *Cartography and Geographic Information Science*, 37(1), 57–68.

Sutley, E. J. and Hamideh, S. (2018). "An interdisciplinary system dynamics model for post-disaster housing recovery." *Sustainable and Resilient Infrastructure*, 3(3), 109–127.

Sutley, E. J. and Hamideh, S. (2020). "Postdisaster Housing Stages: A Markov Chain Approach to Model Sequences and Duration Based on Social Vulnerability." *Risk Analysis*, 40(12), 2675–2695.

Triveño, L., Ijjász-Vásquez, E., Gosling-Goldsmith, J., and Cortés, C. A. (2025). "Housing policies for the new paradigm: Lessons learned from World Bank disaster recovery projects (1980–2024)." *International Journal of Disaster Risk Reduction*, 130, 105871.

U.S. Census Bureau (2021). "Building permits survey: Frequently asked questions. https://www.census.gov/construction/bps/faqs.html. Accessed February 2026.

U.S. Census Bureau (2025a). "Building permits survey. https://www.census.gov/construction/bps/. Accessed February 2026.

U.S. Census Bureau (2025b). "Building permits survey: Methodology. https://www.census.gov/construction/bps/methodology.html. Accessed February 2026.

U.S. Department of Housing and Urban Development (2006). "Current housing unit damage estimates: Hurricanes Katrina, Rita, and Wilma." *Report no.*, U.S. Department of Housing and Urban Development. https://www.huduser.gov/publications/pdf/gulfcoast_hsngdmgest.pdf. Accessed March 2026.

van de Lindt, J. W., Peacock, W. G., Mitrani-Reiser, J., Rosenheim, N., Deniz, D., Dillard, M., Tomiczek, T., Koliou, M., Graettinger, A., Crawford, P. S., et al. (2020). "Community resilience-focused technical investigation of the 2016 Lumberton, North Carolina flood: Multi-disciplinary approach." *Natural Hazards Review*, 21(3), 04020029.

Ventura (2026). "Thomas Fire Information | Ventura, CA.

Wang, W. and van de Lindt, J. W. (2021). "Quantitative modeling of residential building disaster recovery and effects of pre- and post-event policies." *International Journal of Disaster Risk Reduction*, 59, 102259.

SUPPLEMENTAL MATERIALS FOR SINGLE-FAMILY RESIDENTIAL RECONSTRUCTION AFTER DISASTERS: BUILDING PERMITS SURVEY DATA AND SYNTHETIC CONTROLS

Supplemental figures

Figure S1 shows the nation-wide counts of building permits from the considered data set. The data shows strong macroeconomic trends (e.g., the pre-2008 housing boom and subsequent crash), and seasonality, motivating the use of synthetic controls to normalize for these effects.

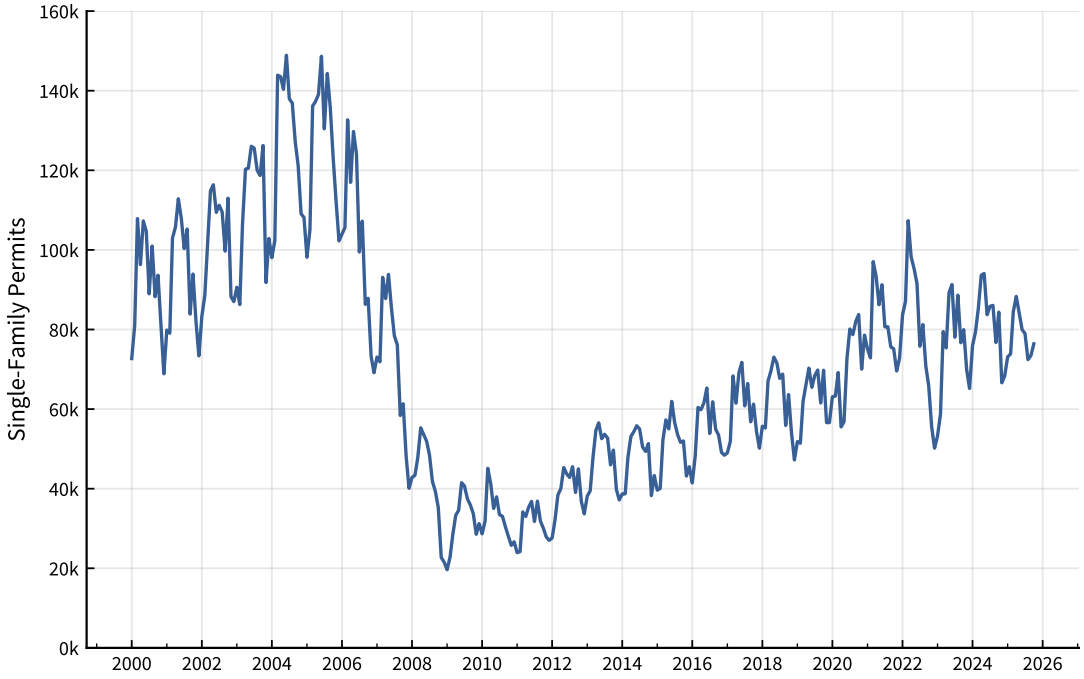

Fig. S1. Time series of BPS single-family building permits for all places and dates in the considered data set.

Figure S2 shows the number of donors with non-zero weights (Eq. 1) for each disaster-affected place. The number of donors ranges from 6 to 32, with a median of 13.

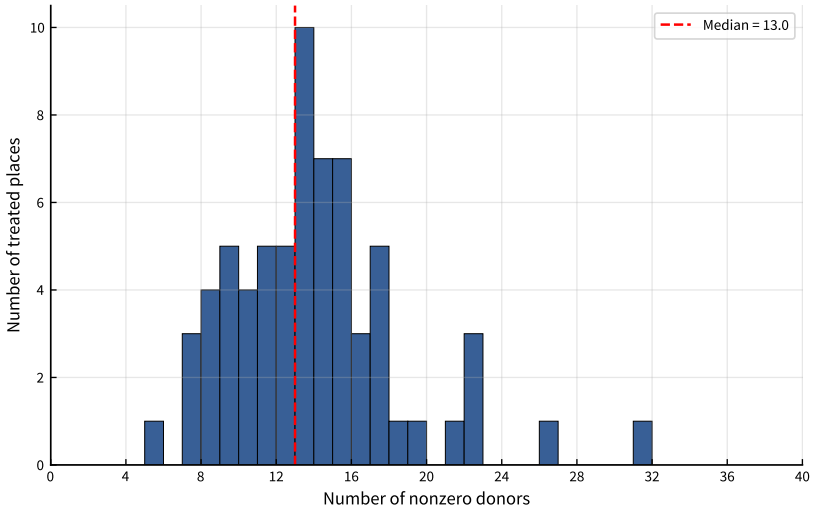

Fig. S2. Distribution of the number of nonzero donor weights across the 67 considered disaster-affected places.

Figure S3 shows the source states for synthetic control donors. Each row represents a state with disaster-affected places (n indicates the number of places). Each column represents a state with donor places. Cell shading and labels indicate the percentage of donor places coming from the state in that column. Because donors were only considered from within a Census Region, the affected places and donors can be grouped by Region. Donors from the disaster-affected state were excluded by rule.

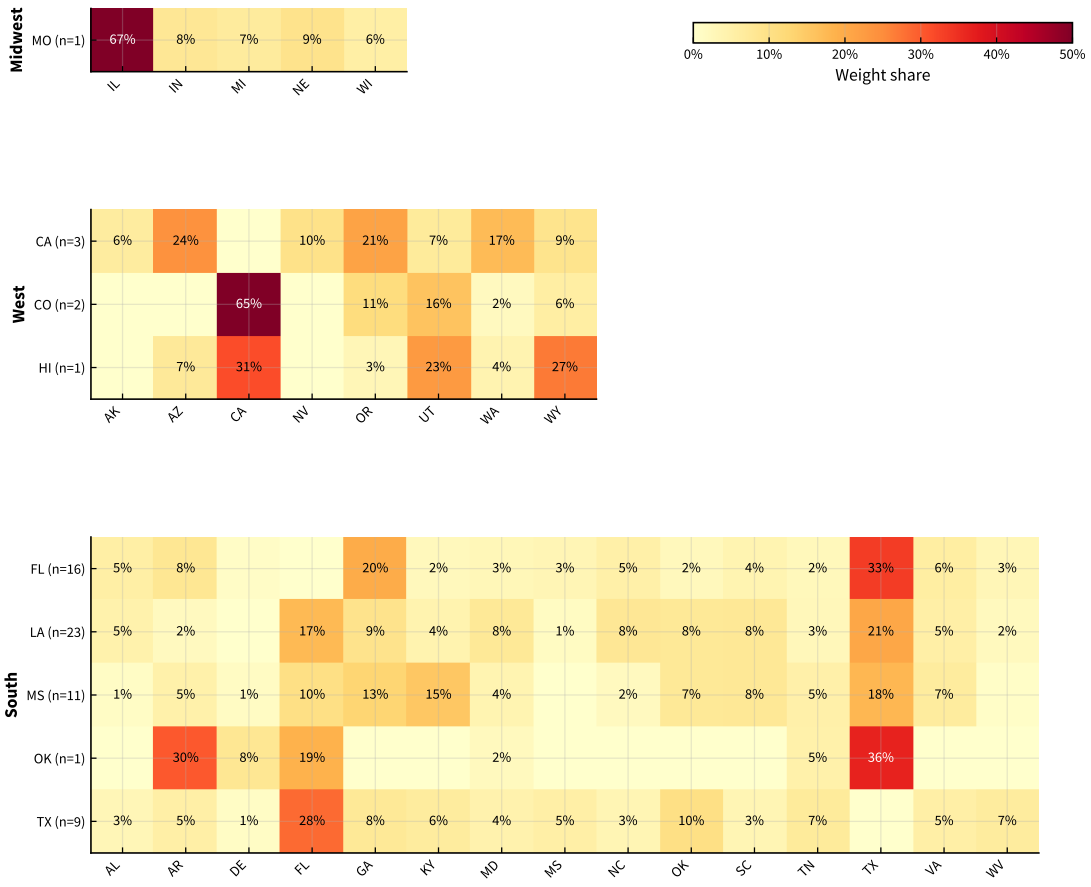

Fig. S3. Share of total donor weight by state, aggregated across treated places in each treated state. Both axes are sorted by Census region (West, South, Midwest), revealing a block-diagonal pattern: donors are drawn from other states in the same Census region, as specified by the donor pool construction. Cell values show the percentage of total weight contributed by each donor state; states contributing less than 5% in all rows are omitted.

Figures S4 through S15 show the individual actual-versus-synthetic time series for all 67 fitted places, grouped by disaster type. Thin lines show raw monthly permit counts; bold lines show 12-month moving averages. Gray dashed lines show the synthetic control. Red dashed vertical lines mark disaster dates with FEMA IA statistics (registrations and assessed damage). Purple dotted lines mark excluded second events for places affected by two hurricanes in the study period. Gray shading indicates periods when the place was absent from the BPS monthly survey.

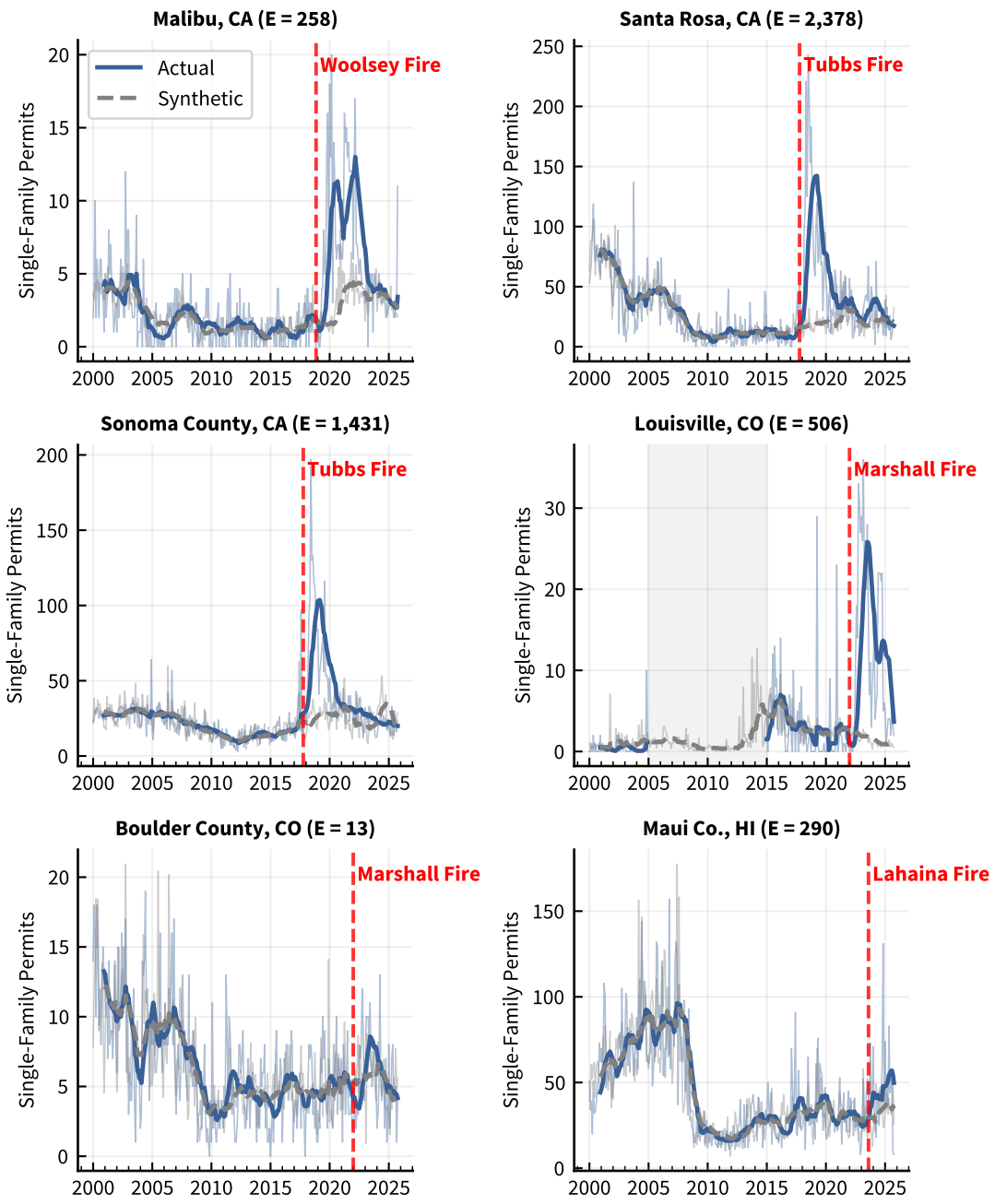

Fig. S4. Wildfire places: actual vs. synthetic single-family permits. Thin lines show raw monthly data; bold lines show 12-month moving averages. Red dashed lines mark disaster dates. Gray shading indicates BPS survey gaps.

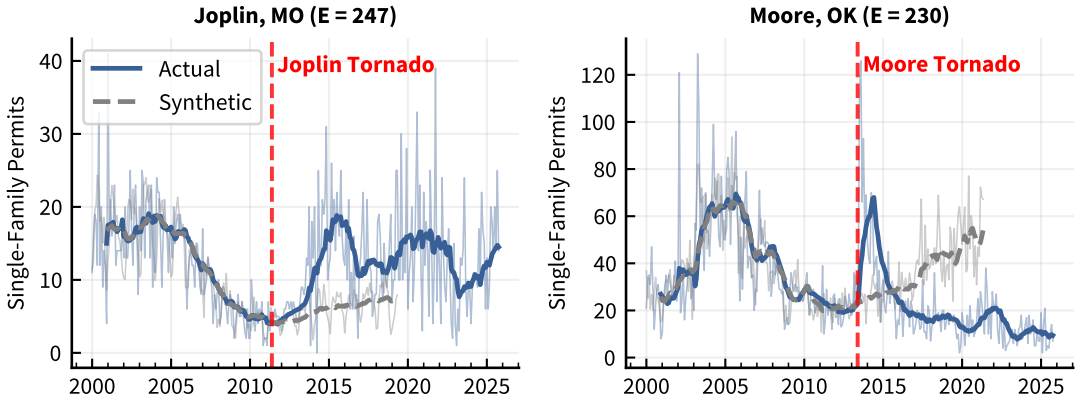

Fig. S5. Tornado places: actual vs. synthetic single-family permits. Thin lines show raw monthly data; bold lines show 12-month moving averages. Red dashed lines mark disaster dates.

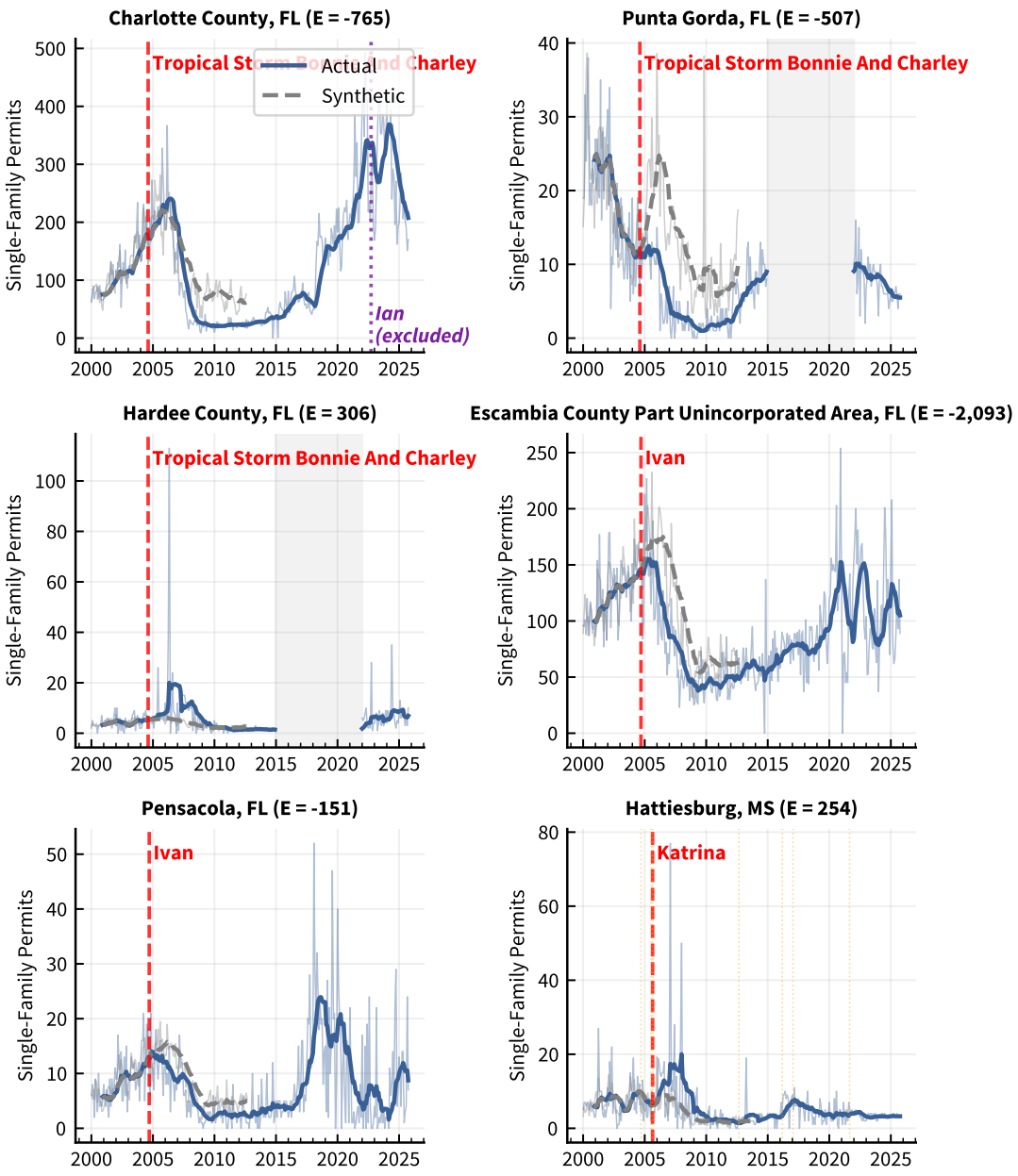

Fig. S6. Hurricane places (1 of 10): actual vs. synthetic single-family permits. Red dashed lines mark disaster dates. Purple dotted lines mark excluded second hurricane events. Gray shading indicates BPS survey gaps.

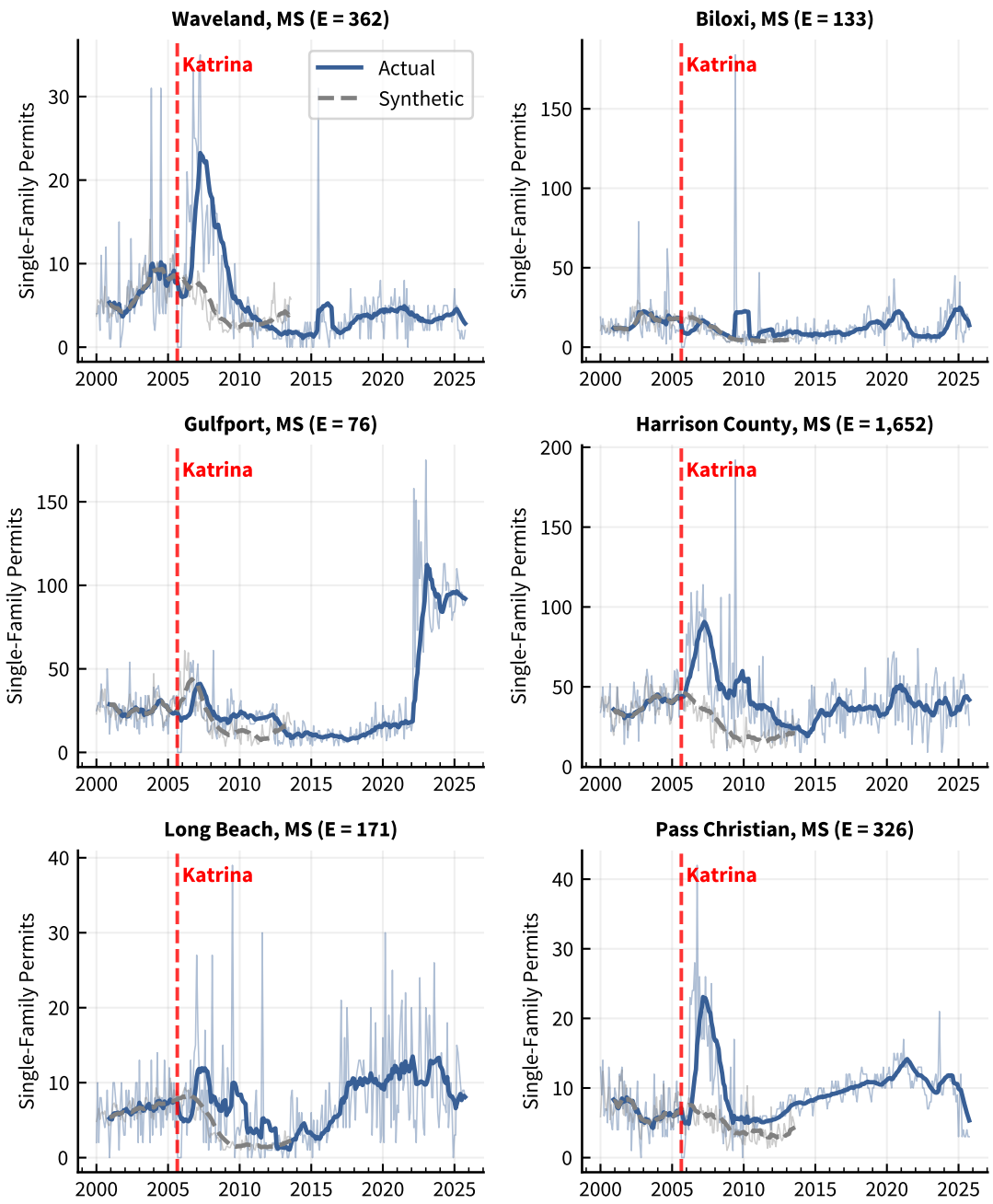

Fig. S7. Hurricane places (2 of 10).

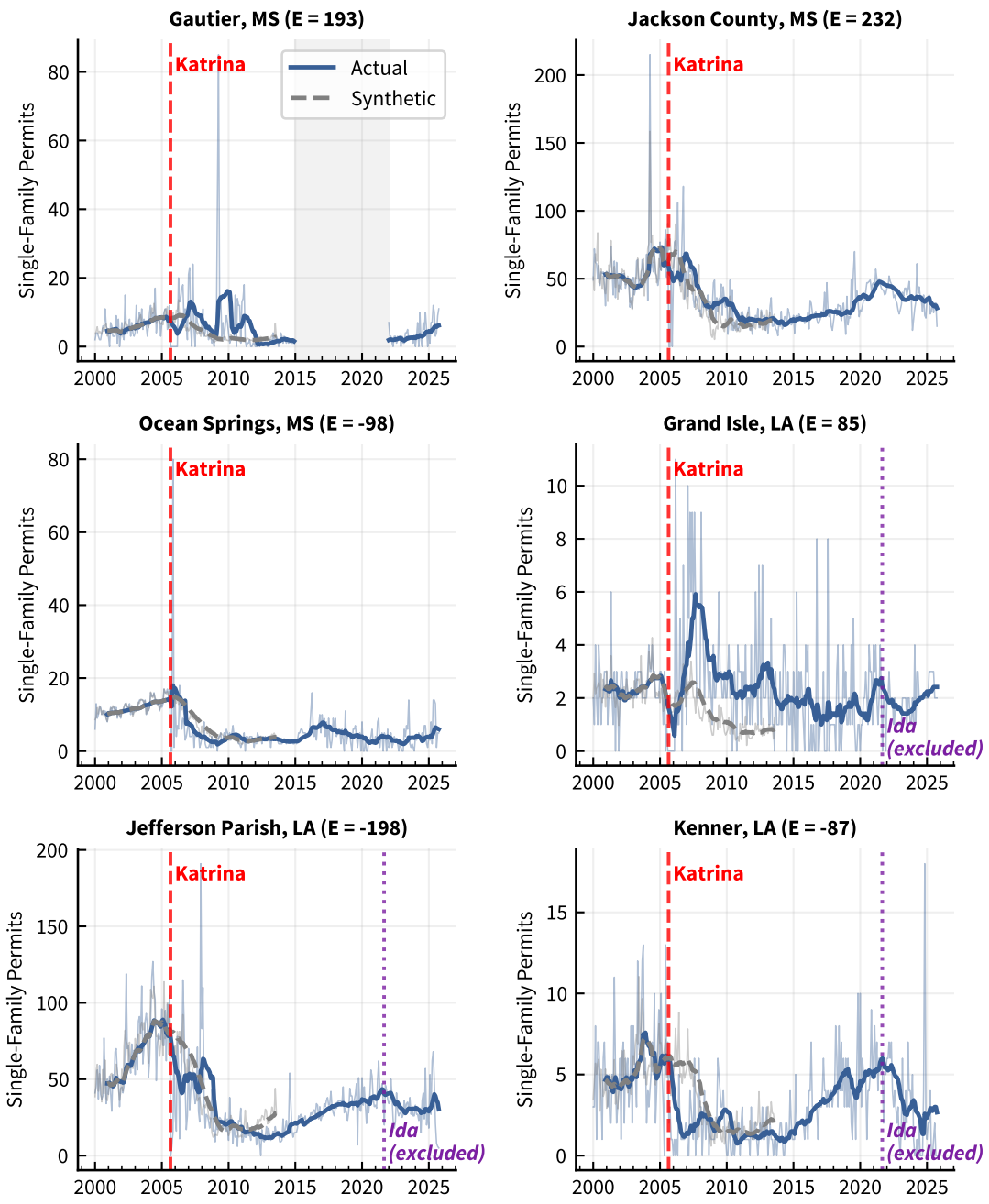

Fig. S8. Hurricane places (3 of 10).

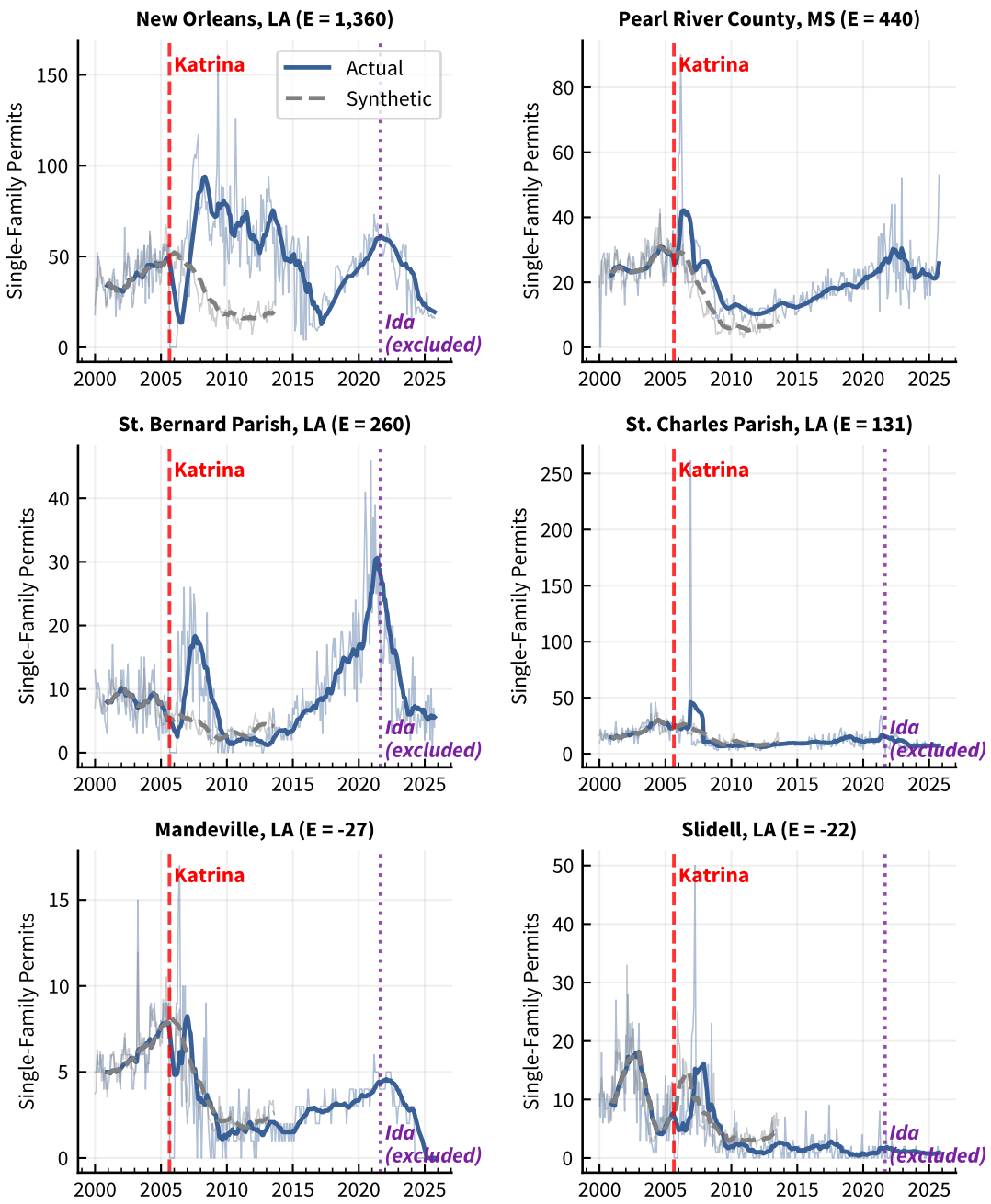

Fig. S9. Hurricane places (4 of 10).

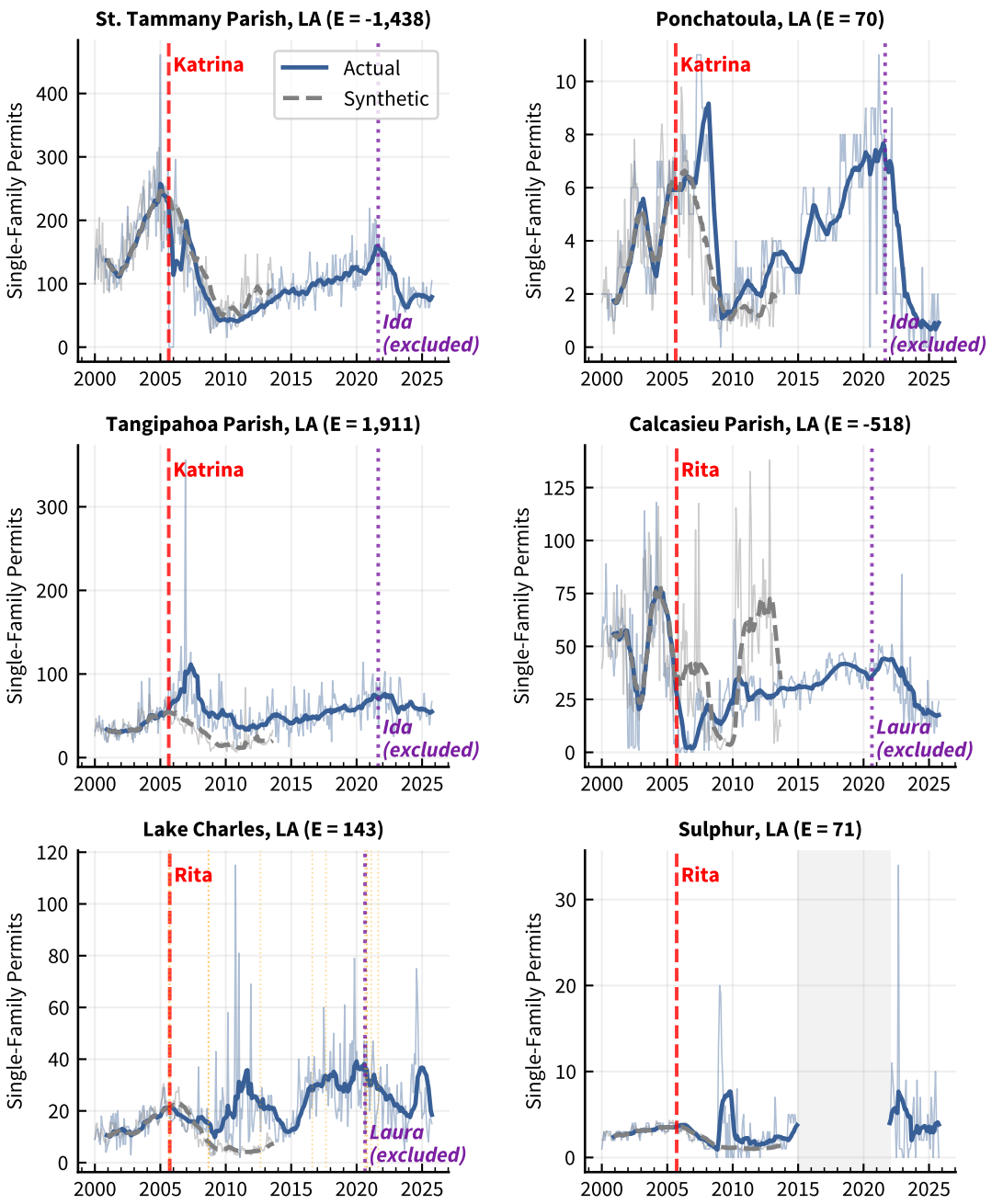

Fig. S10. Hurricane places (5 of 10).

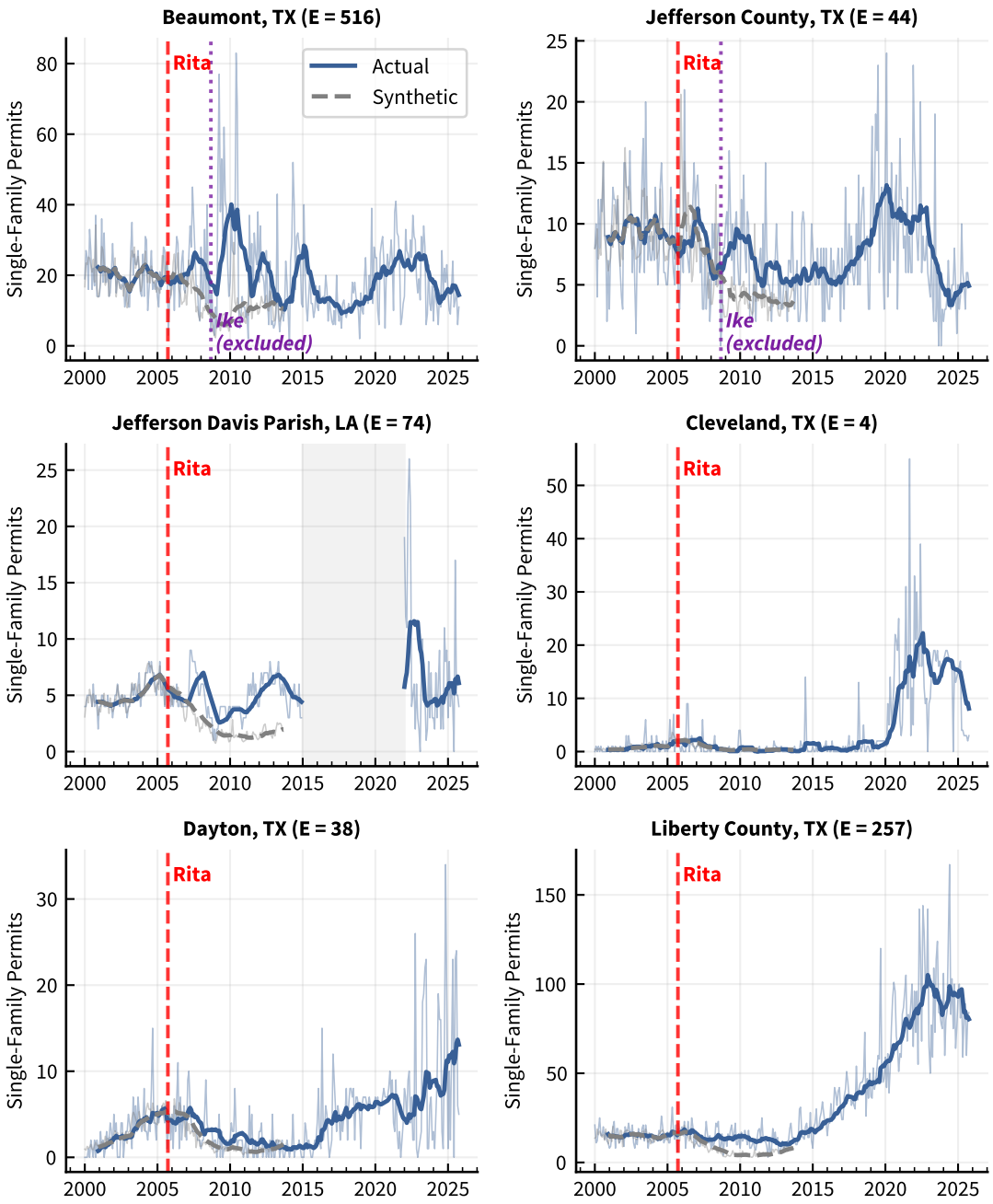

Fig. S11. Hurricane places (6 of 10).

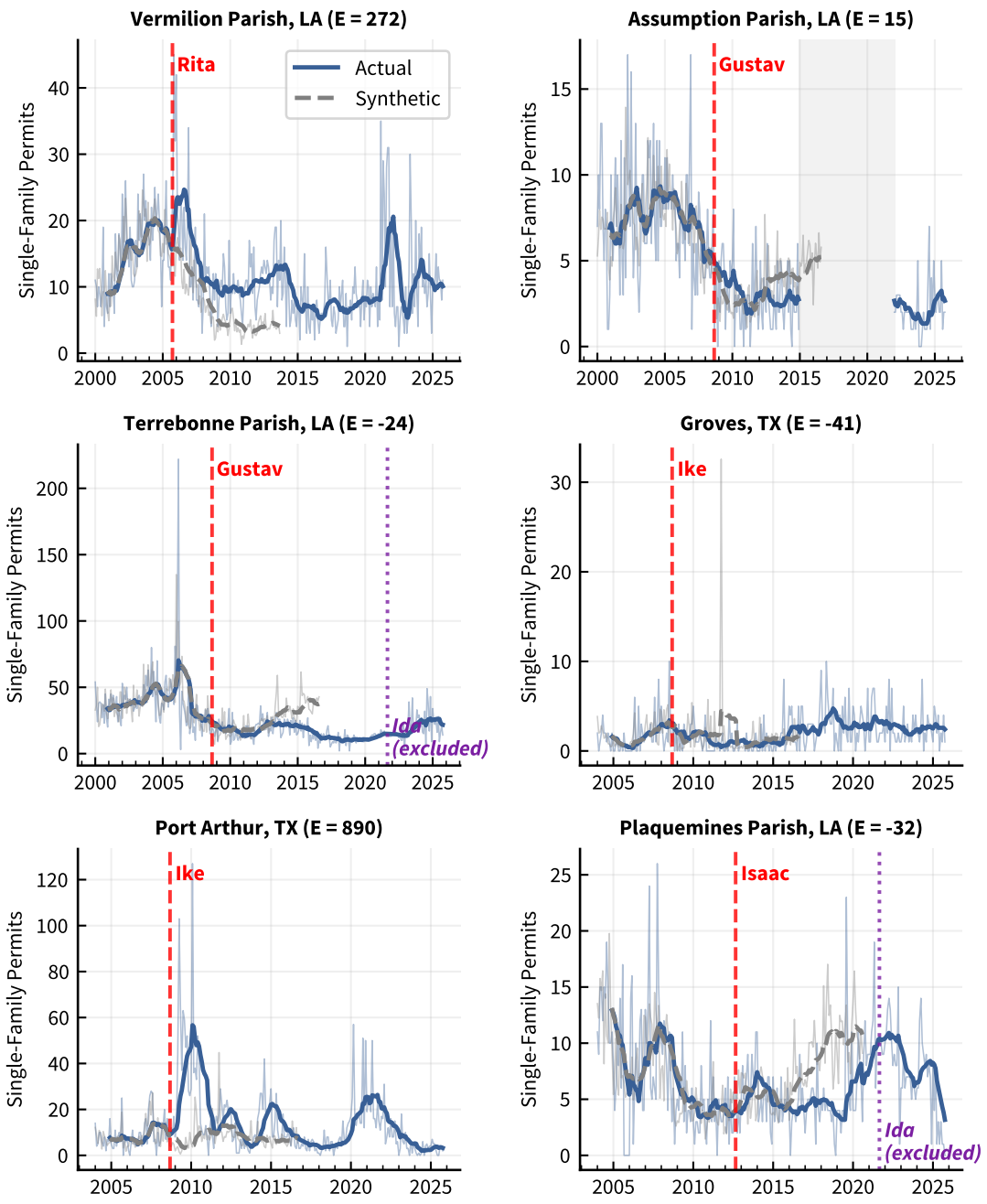

Fig. S12. Hurricane places (7 of 10).

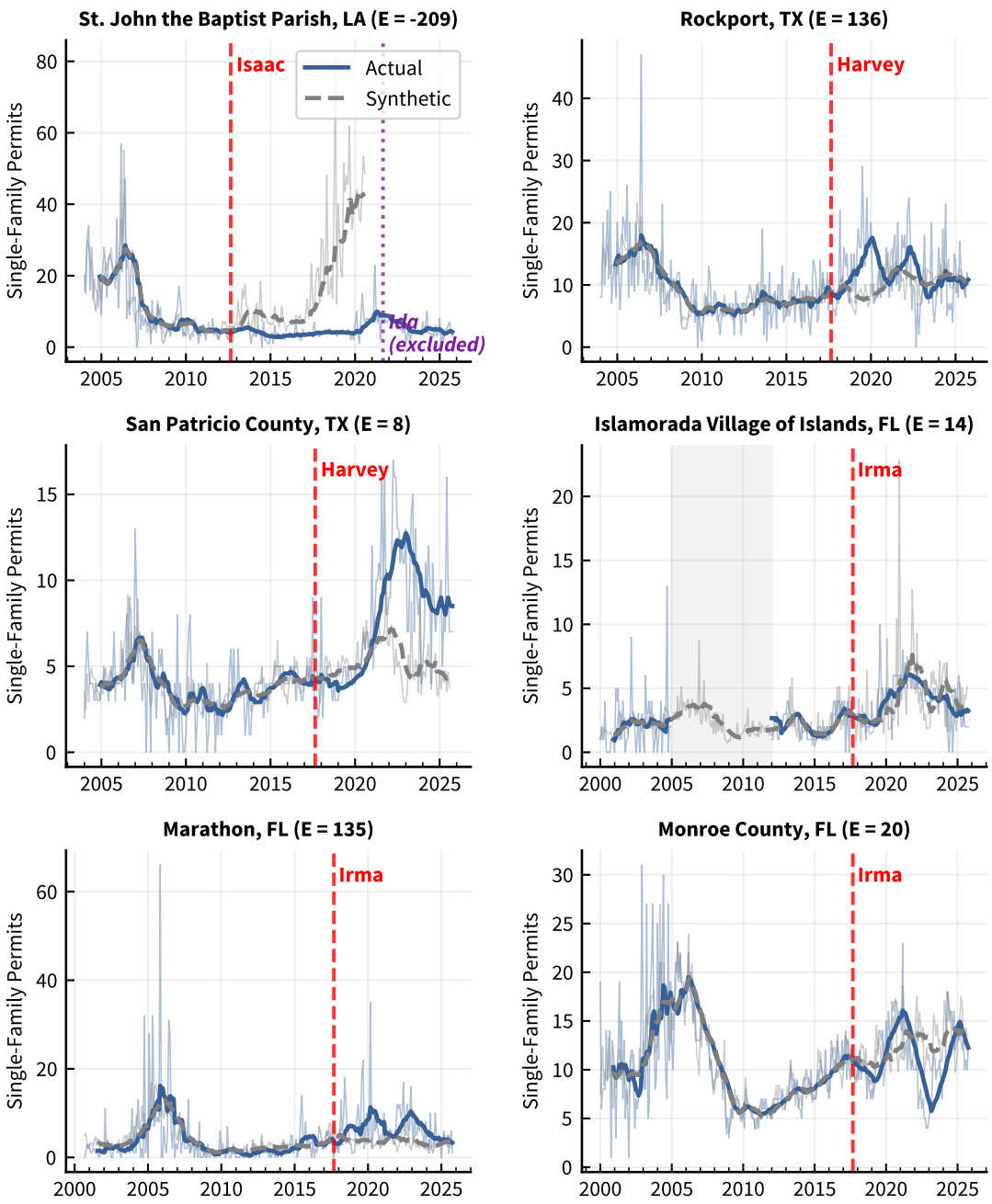

Fig. S13. Hurricane places (8 of 10).

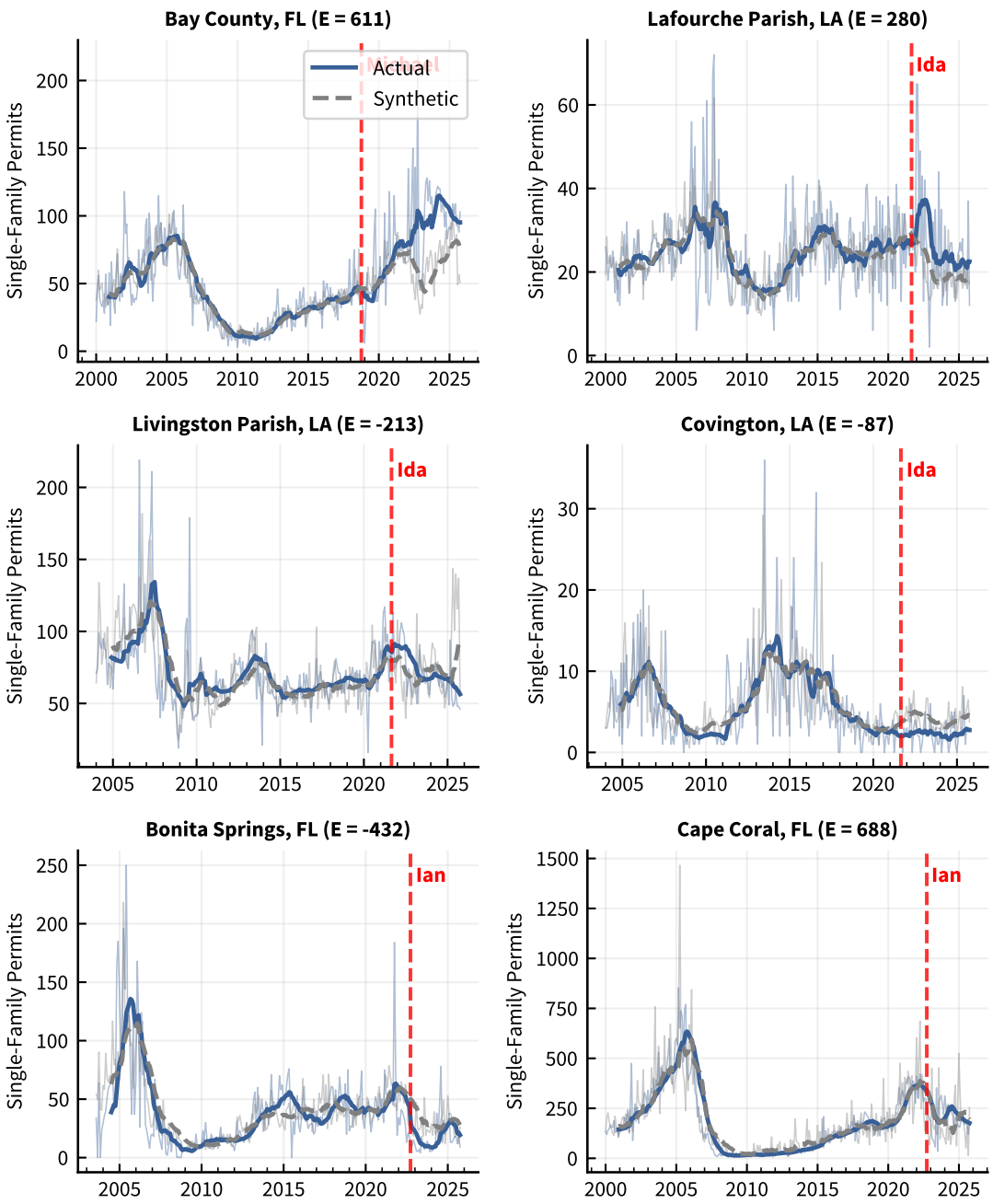

Fig. S14. Hurricane places (9 of 10).

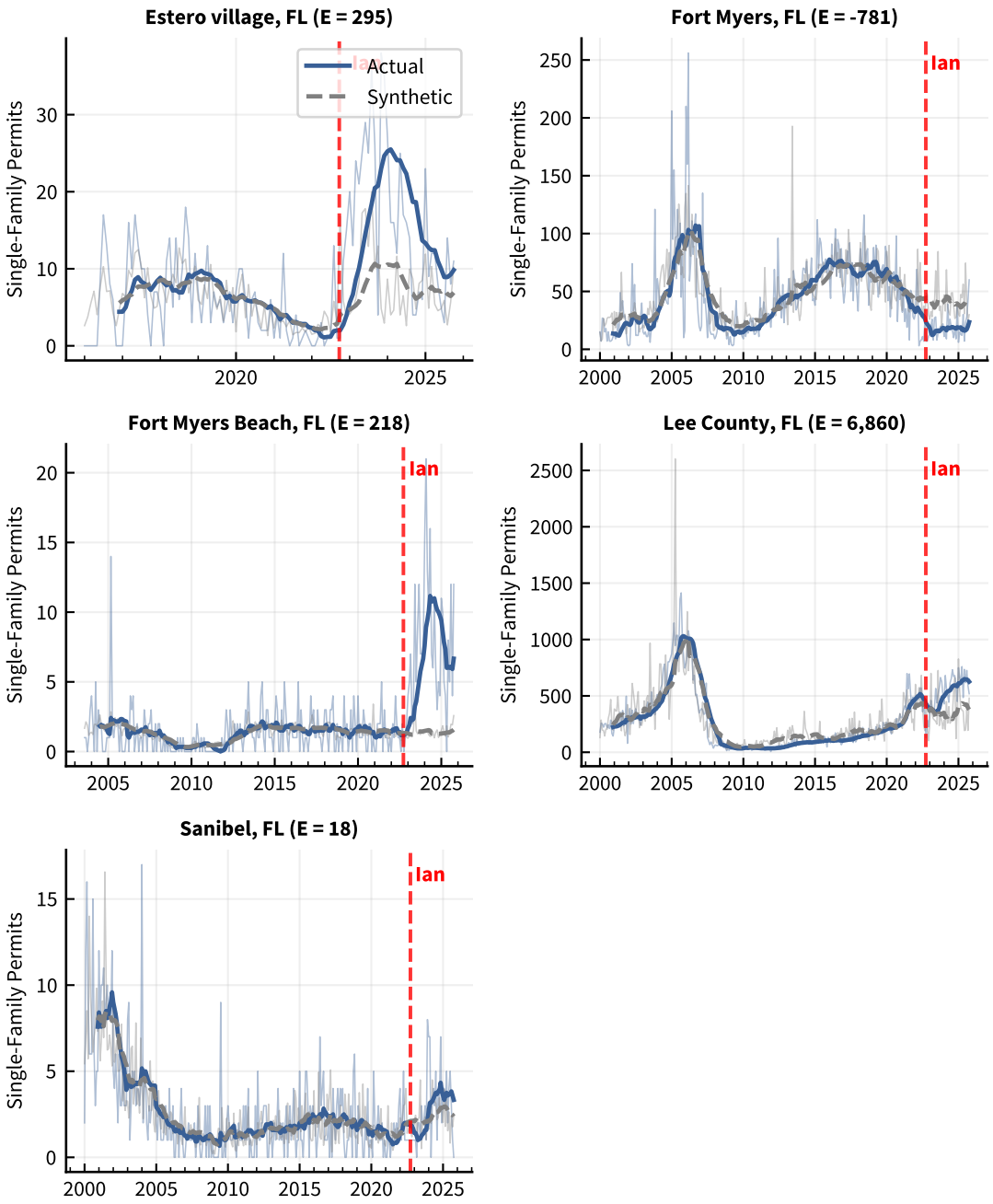

Fig. S15. Hurricane places (10 of 10).

Figures S16 and S17 show time series for wildfires and earthquakes that were considered but excluded from analysis. Most have BPS survey gaps adjacent to the disaster event, and Ventura has evidence of reporting inconsistencies, as discussed in the paper. No synthetic controls were produced due to these data issues, and so none are shown on the figures.

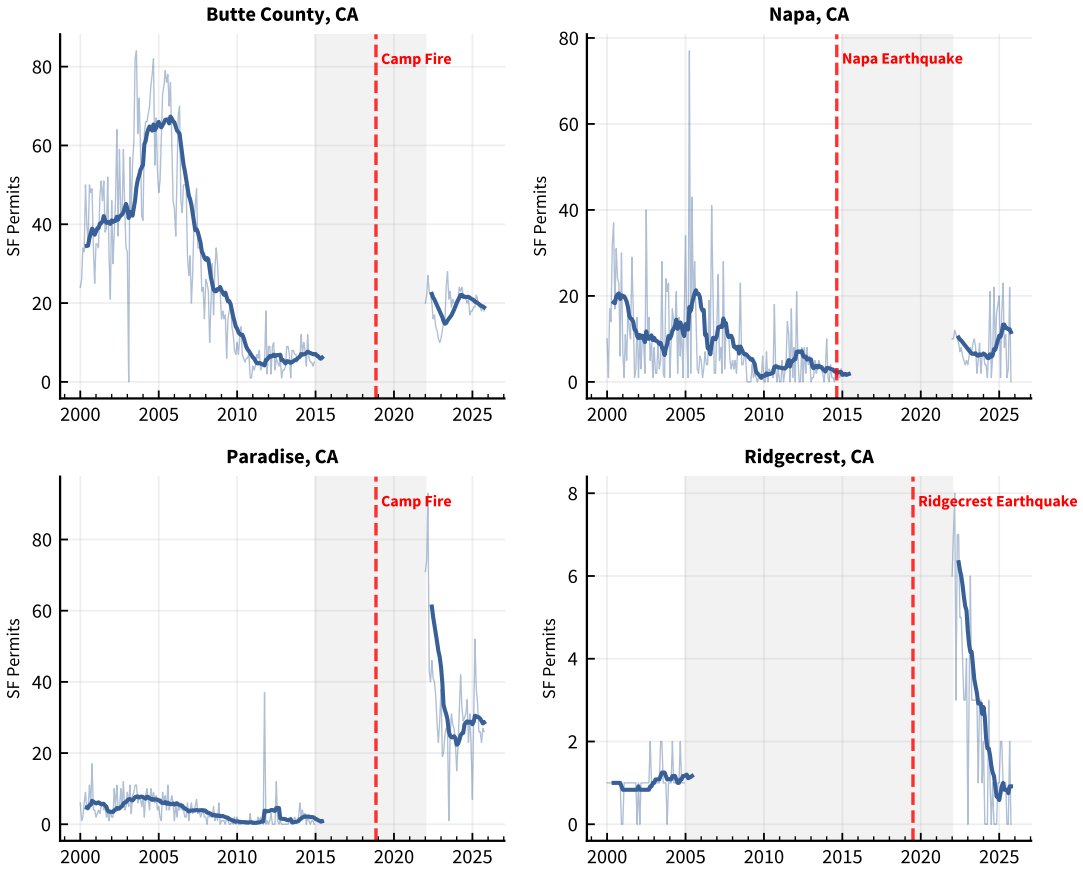

Fig. S16. Excluded places (1 of 2): Raw single-family permit time series for the places that were considered but excluded from the synthetic control analysis due to BPS survey limitations (data gaps or reporting inconsistencies).

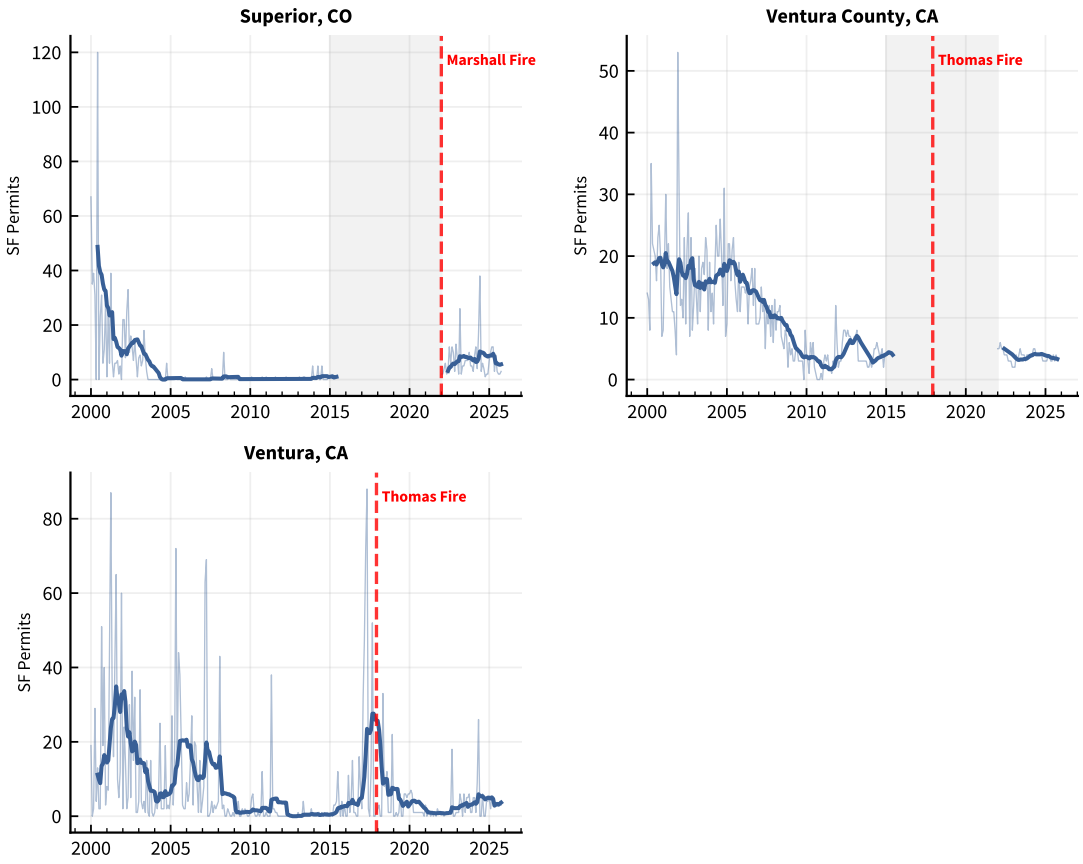

Fig. S17. Excluded places (2 of 2).

Supplemental table

Table 2 summarizes the computed Excess Permits for each considered place, and the reported number of destroyed buildings in each place, with sources for the reported numbers. These results are provided for reference, but a number of significant limitations should be noted:

1. **Geographic scope mismatches.** Several figures are county- or parish-level totals rather than place-level counts. For example, the Harrison County figure (7,618) aggregates destruction across Gulfport, Biloxi, Long Beach, and Pass Christian; the Jefferson Parish figure (4,677) encompasses Kenner and surrounding communities.
2. **Structure type.** Some figures count all structure types (residential, commercial, and other), while others count residential structures only. CAL FIRE damage inspection totals are all-structure counts. Marshall Fire figures are residential only, per the Boulder County Office of Disaster Management assessment. The Joplin Tornado figure (3,181) is the number of residential structures assessed as destroyed in the NIST technical investigation.
3. **Definition of "destroyed."** Damage-state classifications differ across sources. CAL FIRE uses its own post-fire inspection categories; the HUD Gulf Coast report uses "Severe" damage as the proxy for destroyed; and NHC tropical cyclone reports use FEMA damage assessment classifications.
4. **Lower-bound estimates.** The NHC report for Hurricane Michael states that more than

1,500 structures were destroyed in Bay County; the reported value is therefore a lower bound rather than a precise count.

5. **Missing values.** Many hurricane-affected places have no destruction count in the table. Sometimes this is due to a lack of identifiable source, and sometimes because the damage was predominantly repairable and no reliable "destroyed" count is available from standard post-event assessments. This absence of data is somewhat consistent with hurricane damage being less visible to new-construction permit records.

Table 2. Excess building permits and reported structures destroyed for disaster-affected places.

Place	Disaster	E	Destroyed	Source
Santa Rosa (CA)	Tubbs Fire	2,378	3,043	https://www.srcity.org/DocumentCenter/View/24254/Summary-of-Residential-Destruction-Resulting-from-October-2017-Wildfires_41919
Sonoma Co. (CA)	Tubbs Fire	1,431	5,636	https://www.fire.ca.gov/incidents/2017/10/8/tubbs-fire-central-lnu-complex
Malibu (CA)	Woolsey Fire	258	488	https://malibupermits.ci.malibu.ca.us/WoolseyRebuildStats.aspx?returnId=901
Louisville (CO)	Marshall Fire	506	550	https://bouldercounty.gov/news/boulder-county-releases-updated-list-of-structures-damaged-and-destroyed-in-the-marshall-fire/
Boulder Co. (CO)	Marshall Fire	13	156	https://bouldercounty.gov/news/boulder-county-releases-updated-list-of-structures-damaged-and-destroyed-in-the-marshall-fire/
Maui Co. (HI)	Lahaina Fire	290	2,207	https://www.mauicounty.gov/m/newsflash/Home/Detail/12683?arc=17713
Joplin (MO)	Joplin Tornado	247	3,181	https://nvlpubs.nist.gov/nistpubs/NCSTAR/NIST.NCSTAR.3.pdf
Moore (OK)	Moore Tornado	230	1,128	https://nvlpubs.nist.gov/nistpubs/SpecialPublications/NIST.SP.1164.pdf
Charlotte Co. (FL)	Bonnie & Charley	-765	—	
Hardee Co. (FL)	Bonnie & Charley	306	—	
Punta Gorda (FL)	Bonnie & Charley	-507	—	
Escambia Co. (FL)	Ivan	-2,093	—	
Pensacola (FL)	Ivan	-151	—	
Grand Isle (LA)	Katrina	85	—	
Jefferson Par. (LA)	Katrina	-198	4,677	https://www.huduser.gov/publications/pdf/gulfcoast_hsngdmgest.pdf
Kenner (LA)	Katrina	-87	—	
Mandeville (LA)	Katrina	-27	—	
New Orleans (LA)	Katrina	1,360	—	
Ponchatoula (LA)	Katrina	70	—	
Slidell (LA)	Katrina	-22	—	
St. Bernard Par. (LA)	Katrina	260	13,748	https://www.huduser.gov/publications/pdf/gulfcoast_hsngdmgest.pdf

Place	Disaster	E	Destroyed	Source
St. Charles Par. (LA)	Katrina	131	51	https://www.huduser.gov/publications/pdf/gulfcoast_hsngdmgest.pdf
St. Tammany Par. (LA)	Katrina	-1,438	1,682	https://www.huduser.gov/publications/pdf/gulfcoast_hsngdmgest.pdf
Tangipahoa Par. (LA)	Katrina	1,911	130	https://www.huduser.gov/publications/pdf/gulfcoast_hsngdmgest.pdf
Biloxi (MS)	Katrina	133	—	
Gautier (MS)	Katrina	193	—	
Gulfport (MS)	Katrina	76	—	
Harrison Co. (MS)	Katrina	1,652	7,618	https://www.huduser.gov/publications/pdf/gulfcoast_hsngdmgest.pdf
Hattiesburg (MS)	Katrina	254	—	
Jackson Co. (MS)	Katrina	232	2,043	https://www.huduser.gov/publications/pdf/gulfcoast_hsngdmgest.pdf
Long Beach (MS)	Katrina	171	—	
Ocean Springs (MS)	Katrina	-98	—	
Pass Christian (MS)	Katrina	326	—	
Pearl River Co. (MS)	Katrina	440	218	https://www.huduser.gov/publications/pdf/gulfcoast_hsngdmgest.pdf
Waveland (MS)	Katrina	362	—	
Calcasieu Par. (LA)	Rita	-518	620	https://www.huduser.gov/publications/pdf/gulfcoast_hsngdmgest.pdf
Jefferson Davis Par. (LA)	Rita	74	46	https://www.huduser.gov/publications/pdf/gulfcoast_hsngdmgest.pdf
Lake Charles (LA)	Rita	143	—	
Sulphur (LA)	Rita	71	—	
Vermilion Par. (LA)	Rita	272	207	https://www.huduser.gov/publications/pdf/gulfcoast_hsngdmgest.pdf
Beaumont (TX)	Rita	516	—	
Cleveland (TX)	Rita	4	—	
Dayton (TX)	Rita	38	—	
Jefferson Co. (TX)	Rita	44	321	https://www.huduser.gov/publications/pdf/gulfcoast_hsngdmgest.pdf
Liberty Co. (TX)	Rita	257	56	https://www.huduser.gov/publications/pdf/gulfcoast_hsngdmgest.pdf

Place	Disaster	E	Destroyed	Source
Assumption Par. (LA)	Gustav	15	—	
Terrebonne Par. (LA)	Gustav	-24	—	
Groves (TX)	Ike	-41	—	
Port Arthur (TX)	Ike	890	—	
Plaquemines Par. (LA)	Isaac	-32	—	
St. John the Baptist Par. (LA)	Isaac	-209	—	
Rockport (TX)	Harvey	136	30% destroyed	https://www.weather.gov/crp/hurricane_harvey
San Patricio Co. (TX)	Harvey	8	580	https://www.weather.gov/crp/hurricane_harvey
Islamorada (FL)	Irma	14	—	
Marathon (FL)	Irma	135	—	
Monroe Co. (FL)	Irma	20	727	https://www.monroecounty-fl.gov/726/Hurricane-Irma-Recovery
Bay Co. (FL)	Michael	611	1,500	https://www.nhc.noaa.gov/data/tcr/AL142018_Michael.pdf
Covington (LA)	Ida	-87	—	https://www.nhc.noaa.gov/data/tcr/AL092021_Ida.pdf
Lafourche Par. (LA)	Ida	280	—	
Livingston Par. (LA)	Ida	-213	—	
Bonita Springs (FL)	Ian	-432	—	
Cape Coral (FL)	Ian	688	—	
Estero (FL)	Ian	295	—	
Fort Myers (FL)	Ian	-781	—	
Fort Myers Beach (FL)	Ian	218	900	https://www.nhc.noaa.gov/data/tcr/AL092022_Ian.pdf
Lee Co. (FL)	Ian	6,860	5,369	https://www.nhc.noaa.gov/data/tcr/AL092022_Ian.pdf
Sanibel (FL)	Ian	18	—	https://www.nhc.noaa.gov/data/tcr/AL092022_Ian.pdf